https://doi.org/10.5194/egusphere-2024-1468
Preprint. Discussion started: 30 May 2024

AdriE: a high-resolution ocean model ensemble for the Adriatic Sea under severe climate change conditions

Davide Bonaldo[1], Sandro Carniel[2,a], Renato R. Colucci[2,b], Cléa Denamiel[3,4], Petra Pranić[5], Fabio Raicich[6], Antonio Ricchi[7,8], Lorenzo Sangelantoni[9], Ivica Vilibić[3,4], and Maria Letizia Vitelletti[1]

[1]National Research Council of Italy, Institute of Marine Sciences (CNR-ISMAR), Venice, Italy
[2]National Research Council of Italy, Institute of Polar Sciences, (CNR-ISP), Venice, Italy
[a]currently at: NATO STO Centre for Maritime Research and Experimentation, La Spezia, Italy
[b]previously at: CNR-ISMAR, Trieste, Italy
[3]Ruder Bošković Institute, Division for Marine and Environmental Research, Zagreb, Croatia
[4]Institute of Adriatic Crops and Karst Reclamation, Split, Croatia
[5]Institute of Oceanography and Fisheries, Split, Croatia
[6]National Research Council of Italy, Institute of Marine Sciences (CNR-ISMAR), Trieste, Italy
[7]Department of Physical and Chemical Sciences, University of L'Aquila, L'Aquila, Italy
[8]Center of Excellence in Telesensing of Environment and Model Prediction of Severe Events (CETEMPS), University of L'Aquila, L'Aquila, Italy
[9]CMCC Foundation - Euro-Mediterranean Center on Climate Change, Bologna, Italy

Correspondence: Davide Bonaldo (davide.bonaldo@cnr.it)

Abstract. With its complex and peculiar meteo-oceanographic dynamics and the coexistence of diverse socio-economic activities and pressures with outstanding cultural heritage and environmental assets, the Adriatic basin (Mediterranean Sea) has traditionally been considered as a natural laboratory for marine science in its broadest meaning. In recent years the intensification of the effects of climate change, together with the increasing awareness of its possible consequences and of the knowledge gaps hampering a long-term response, have opened new questions and reframed most of the existing ones into a multi-decadal time scale. In this perspective, a description of the possible evolution of the physical oceanographic processes is the baseline for addressing the multi-disciplinary challenges set by climate change, but up to now it has not been possible to combine for this basin a sufficiently high resolution in the process description with an estimate of the uncertainty associated with the predictions. This work presents an end-of-century, kilometre-scale ensemble modelling approach for the description of ocean processes in the Adriatic Sea. Addressing 3-D circulation and thermohaline dynamics within the Regional Ocean Modelling System (ROMS), the ensemble consists of six climate runs encompassing the period from 1987 to 2100 in a severe RCP8.5 scenario forced by the SMHI-RCA4 Regional Climate Model, driven by as many different CMIP5 General Climate Models made available within the EURO-CORDEX Initiative. The climate ensemble is flanked by a dedicated evaluation run for the 1987-2010 period, in which SMHI-RCA4 has been driven by reanalysis fields approximating the better available boundary conditions, thus isolating the intrinsic sources of uncertainty of the RCA4-ROMS modelling chain. In order to allow a direct comparison, the assessment of the model skills in the evaluation run borrows, as far as possible, data and approaches used for the evaluation of a recent kilometre-scale, multi-decadal modelling effort for this region. The model performances are mostly aligned with the state-of-art reference, with particularly encouraging results in terms of description of Marine Heat Waves and

https://doi.org/10.5194/egusphere-2024-1468
Preprint. Discussion started: 30 May 2024

Cold Spells. Future projections suggest an increase in temperature and salinity at upper and intermediate depths, resulting in an overall decrease in water density and possibly in deep ventilation rates. Projected variations are stronger in summer and autumn, and in these seasons the ensemble range is larger than the spatial variability of the quantities and occasionally comparable with the intensity of the climate signal, highlighting the importance of an ensemble approach to treat the climate variability at this time scale. Monthly averages of the main quantities are available for each run on a dedicated Zenodo repository, and subsets of the full modelling dataset can be requested to the corresponding author.

1 Introduction

The Adriatic Sea is a semi-enclosed sub-basin of the eastern Mediterranean Sea, elongating along the NW-SE direction and surrounded along its major axis (approximately 800 km) by the Apennines and the Balkans, and closed on its northern end by the Padan-Venetian-Friulian plain. The basin is characterised by a broad and shallow continental shelf, crossed along the SW-NE direction at approximately 43 °N by the Jabuka Pit (maximum depth 280 m) and eventually plunging into the southern Adriatic Pit (SAP) between the Apulia peninsula and the Montenegro-Albanian coast. The SAP, whose depth ranges between 180 m at the continental shelf edge and 1200 at its deepest point, is connected to the Ionian sea through the Otranto strait and its 780-metre deep sill (Orlić et al., 1992; Bonaldo et al., 2016).

Due to the coexistence of manifold meteo-oceanographic processes and different socio-economical pressures and interests, the Adriatic Sea is traditionally regarded as a natural oceanographic laboratory for diverse applications. For instance, the presence of highly-exposed sites of outstanding natural and cultural value and long stretches of low-lying sandy beaches has been a key motivation for studies on coastal erosion (Bonaldo et al., 2019, and references therein) and flooding (Vilibić et al., 2017), and on the physical drivers of these events. Furthermore, the challenges related to the basin morphology and its orographic configuration have motivated numerical modelling and EO analysis developments for coastal regions (Sanchez-Arcilla et al., 2021; Umgiesser et al., 2022). The importance of the Adriatic Sea as a cold engine for the Mediterranean thermohaline circulation (Bergamasco and Malanotte-Rizzoli, 2010) has fostered fecund research lines on dense water formation, deep ventilation, and the relations of these processes with continental margin geomorphology and deep-sea ecology (Bonaldo et al., 2016; Bargain et al., 2018; Vilibić et al., 2023). In recent years, climate change and its effects have progressively gained prominency in this scene, increasingly calling for the projection of the possible evolution of marine systems in this basin over a multi-decadal time scale at a sufficient level of detail. While the predominantly coastal setting of the Adriatic basin demands a high-resolution modelling approach, the temporal range of the processes related to climate change requires a multi-decadal coverage. In this direction some efforts have been undertaken at first for wind waves and barotropic dynamics (Benetazzo et al., 2012; Lionello et al., 2012; Bonaldo et al., 2020). Subsequently, recent achievement in terms of high-resolution, three-dimensional ocean modelling was reached by the AdriSC modelling suite (**?**Denamiel et al., 2021a), in which kilometre-scale projections of trends, variability and extremes in both atmosphere and ocean have been achieved (Tojčić et al., 2024), but only for one climate scenario (RCP 8.5) and for far-future period (2070-2100). At these scales, running a climate model is requiring enormous computational resources, thus the full scenario simulation was not affordable and pseudo-global warming approach has been

https://doi.org/10.5194/egusphere-2024-1468
Preprint. Discussion started: 30 May 2024

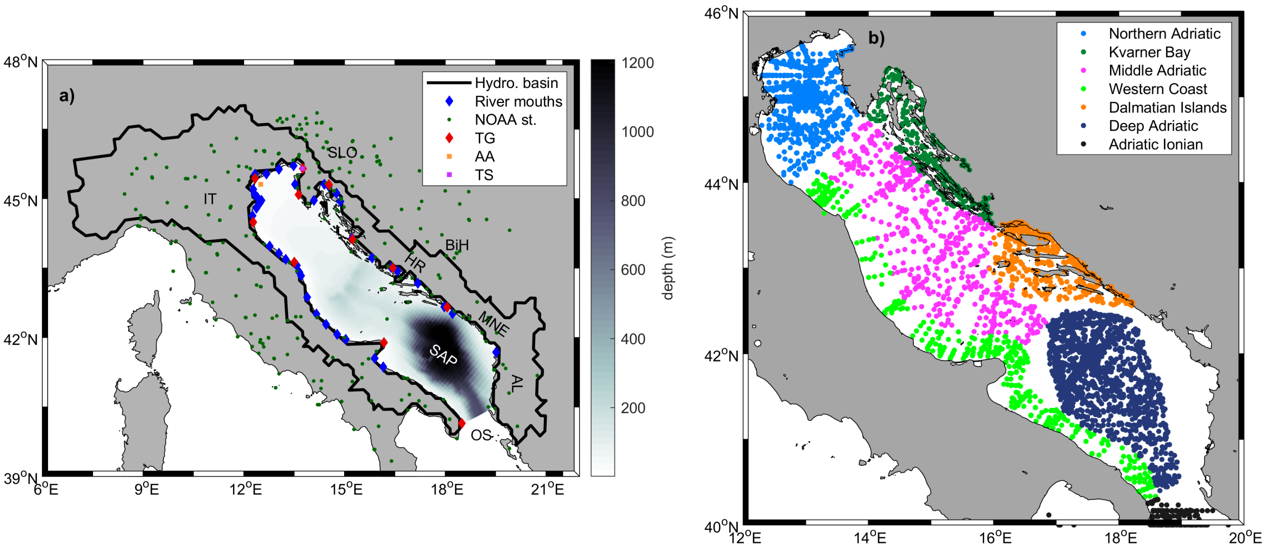

Figure 1. Geographical setting. a) Model domain and bathymetry of the AS, with indication of the NOAA stations and of the tide gauges (TG) considered in the validation, as well as the position of the Acqua Alta (AA) and Trieste (TS) monitoring stations. The thick black line indicates the hydrographic basin draining into the AS, and the blue diamonds represent the position of the freshwater inputs included in the model. OS represents the open boundary at the Otranto Strait. b) Position of the CTD measurements and identification of the subdomains described by Pranić et al. (2021).

implemented and extended to the ocean (Denamiel et al., 2020). Nonetheless, climate change projections are subject to several levels of uncertainty, ranging from the very evolution of the global climate to how the signal propagates through different scales, alongside with the intrinsic assumptions and approximations in the numerical description of the phenomena to be analysed. This uncertainty is typically addressed by means of ensemble modelling approaches in which the some degrees of freedom are explored by dedicated model runs, but the computational demand of such a task is typically unaffordable outside of a dedicated consortium. On the other hand, such coordinated efforts typically address relatively large spatial scales, failing to capture the local features of climate change. The Med-CORDEX initiative (www.medcordex.eu), although promising over the long shot, is still not providing extensive high-resolution, end-of-century model fields for the Adriatic region, and some shortcomings have been pointed out in the representation of the main thermohaline processes, and particularly in dense water formation (Dunić et al., 2019, 2022). The goal of the present work is to bridge this gap for the Adriatic basin, proposing a trade-off between the very-high resolution required to properly reproduce the local oceanographic processes and the need for an estimate of the uncertainty associated with the future predictions. In this paper we introduce a six-member ocean model ensemble for the Adriatic Sea up to the end of century in the severe climate change scenario RCP8.5 (Church et al., 2013), assessing its performance and discussing the potential and the possible limitations for its applicability in the analysis of the physical oceanographic processes of the basin as well as in downscaling applications for local studies or as a source of information for multidisciplinary efforts.

https://doi.org/10.5194/egusphere-2024-1468
Preprint. Discussion started: 30 May 2024

2 Materials and methods

2.1 AdriE ensemble model implementation

The AdriE ensemble is based on a set of implementations of the ROMS modelling system (Haidvogel et al., 2008) over the Adriatic Sea, with an open boundary at the Otranto Strait (Figure 1a). All simulations are forced with 0.11-degree resolution, 6-hourly atmospheric fields (total cloud fraction, relative humidity, sea-level air pressure, precipitation, long- and shortwave radiation, near-surface air temperature, and near-surface wind velocity components) from the SMHI-RCA4 regional climate model (RCM) (Samuelsson et al., 2011) driven by six Global Climate Models (GCMs) from the CMIP5 initiative (Taylor et al., 2012) and listed in Table 1. SMHI-RCA4 has been used as a reference model in consideration of its extensive record of regional-scale climate projections and its performances in reproducing relevant climate processes (which have been found well representative of the CORDEX multi-model ensemble variability, see Kotlarski et al. 2014), as well as of the availability of the relevant variables with the necessary temporal resolution. The climate ensemble consists of six free-running climate simulations bracketing the period 1987-2099, thus including part of the "historical" (1987-2005, based on the observed radiative forcing) period, and future "scenario" (2006-2099, based on projected values of radiative forcing) under the severe RCP8.5. This set of simulations is flanked by an "evaluation" run (EV hereinafter) in which SMHI-RCA4 was driven by the ERA-INTERIM reanalysis (Dee et al., 2011) throughout the 1987-2010 period synchronised, unlike the climate simulations, with the observed day-to-day climate variability. This allows to isolate the RCM-ROMS modelling chain and assess its skills under an approximation of the best available information at the boundary (ideally the "perfect boundary conditions", see Christensen et al. 1997). Conversely, since GCMs are free running models not constrained, once initialised, to the observed state of the climate system components, the analysis of the climate runs allows the assessment of the skills of the whole modelling chain in terms of statistical properties.

Table 1 summarises the main features of the runs performed. To characterise the largest spectrum of uncertainty we opted for maximising the number of GCMs since these exert a larger influence than RCMs on climate change signal variability (Christensen and Kjellström, 2020, 2022). The use of different models entails a broad spectrum of uncertainty sources (different formulations, numerical schemes, dynamical features, etc.), while different realizations of the same model ("r" index) address different, but equally realistic, initial conditions.

The horizontal discretisation follows the orthogonal curvilinear grid used for the wave climate projections described by Bonaldo et al. (2020), composed of 75 × 180 nodes with resolution ranging from approximately 2 km in the northern regions and progressively decreasing to nearly 10 km in the southeasternmost end of the domain, whereas the water column is discretised into 15 terrain-following σ-levels with increasingly larger thickness towards the bottom. Six sub-domains were identified consistently with the work by Pranić et al. (2021), (namely Northern Adriatic, Kvarner Bay, Middle Adriatic, Western Coast, Dalmatian Islands, and Deep Adriatic; the Adriatic-Ionian subdomain lies mostly outside of the model domain and was not considered in this study), based on their thermohaline properties and circulation features (Figure 1b). The bathymetry was reinterpolated from finer-resolution information adopted in previous works (Benetazzo et al., 2014; Bonaldo et al., 2016, 2019)

https://doi.org/10.5194/egusphere-2024-1468
Preprint. Discussion started: 30 May 2024

Table 1. Overview of climate and evaluation runs and driving models for RCM SMHI-RCA4 from EURO-CORDEX. EV and EV* are forced by the same model but distinguished by the use of different versions of the product from which the boundary conditions were retrieved.

Run	Driving GCM	Period	leap years
NCC	NCC-NorESM1-M r1i1p1	1987-2099	N
CNRM	CNRM-CERFACS-CNRM-CM5 r1i1p1	1987-2099	Y
IPSL	IPSL-IPSL-CM5A-MR r1i1p1	1987-2099	N
MPI	MPI-M-MPI-ESM-LR r1i1p1	1987-2099	Y
ICHEC	ICHEC-EC-EARTH r12i1p1	1987-2099	Y
ICHECb	ICHEC-EC-EARTH r3i1p1	1987-2099	Y
EV	ECMWF-ERAINT	1987-2010	Y
EV*	ECMWF-ERAINT	1987-2010	Y

and smoothed as described by Sikirić et al. (2009) in order to prevent the appearance of artifact horizontal pressure gradients and consequent circulation features.

Potential temperature (θ), salinity (S), momentum and sea level were prescribed as boundary conditions at the Otranto Strait and derived from the MFS 1/16° (Simoncelli et al., 2019). For the EV run, daily values were interpolated throughout the cross section, whereas for the climate runs climatological potential temperature and salinity values, computed with reference to the period 1987-2017 were modulated accordingly with the anomalies computed from Med-CORDEX derived CMCC-CM profiles (Scoccimarro et al., 2011) in the norhtheasternmost grid cell of the Ionian Sea. Furthermore, since during the post-processing of the climate runs a new version of MFS was released (1/24°, see Escudier et al. 2020), an additional evaluation run EV* was carried out to assess the impact of the difference between the two versions on the description of the Adriatic Sea dynamics and the possible implications for the climate projections.

River mouths were included as 39 point freshwater sources. Climatological values from Raicich (1994) were used for the main Alpine (Isonzo, Tagliamento, Piave, Brenta, Adige, and Po split into five branches) and Apennine (Reno, Foglia, Metauro, Esino, Musone, Potenza, Chienti, Tronto, Pescara, Sangro, Trigno, Biferno, Cevaro, Ofanto) rivers, as well as for the Drin in the south-eastern Balkans, while the freshwater input from the Venice lagoon drainage basin was taken from Zuliani et al. (2005). For the rivers and submarine springs along the Croatian coast (Mirna, Raša, Rječina, Bakarac, Crikvenica, Zrmanja, Krka, Jadro, Cetina, Neretva, Ombla, and the Senj and Dubrovnik/Kupari hydropower plants) estimates were taken from Janeković et al. (2014), which in turn also relied on Raicich (1994) for the western coast. For the EV and EV* runs, the input from the Po river was computed from the observed discharge at Pontelagoscuro (approximately 80 km upstream, data publicly available at https://simc.arpae.it/dext3r/, SI@SIMC@ARPAE 2022), whereas for the climate runs climatological river discharges were rescaled following the spatially-averaged modelled rainfall anomaly on the Adriatic catchment (Figure 1a). Tides were included only in the EV and EV* runs by considering 15 tidal components from the TPXO dataset (Egbert and Erofeeva, 2002).

https://doi.org/10.5194/egusphere-2024-1468
Preprint. Discussion started: 30 May 2024

Table 2. Overview of the observational datasets used for the validation.

Name	Variables	Spatial coverage	Temporal coverage	Notes
EOBS	R, SLP, T	land, 0.1°	1987-2010, daily	-
TRMM	R	land and sea, 0.25°	1987-2010, daily	3-hourly in the original dataset
CCMP	U, V, UV	land and sea, 0.25°	1987-2010, daily	6-hourly in the original dataset
NOAA	SLP, T, U, V, UV	pointwise, land	1987-2010, daily	hourly in the original dataset
AA	U, V, UV	pointwise, sea (12°30.55′ E, 45°18.8′ N)	daily	hourly in the original dataset
TG	sea level	pointwise	variable	-
AVHRR	SST	0.0417°	1987-2010, daily	-
T2TS	θ	pointwise, 13°45′ E, 45°39′	daily	-
CTD	θ, S	pointwise profiles	variable	-

2.2 Observational datasets and validation approach

The evaluation of the model skills was based on a broad and heterogeneous set of observations for different variables and from different sources (Table 2). In order to maximise the comparability of the results, and as far as it was relevant and consistent with the aim of this study, the analysis used the datasets, quantities and methods from the works by Denamiel et al. (2021a) and Pranić et al. (2021).

E-OBS v21.0 (Cornes et al., 2018) provided gridded data with 0.1-degree resolution for daily rainfall (R), sea-level pressure (SLP), and near-surface temperature (T) over land. Delivered and periodically updated by the Copernicus Climate Change Service, this dataset combines in-situ observations ensembles and is used as a reference for the evaluation of RCMs within the EURO-CORDEX community (Kotlarski et al., 2014; Varga and Breuer, 2020). Additional rainfall data were also collected from the Tropical Rainfall Measuring Mission (TRMM) gridded dataset (Huffman et al., 2016) with 0.25-degree resolution over land and sea, based on the combination of microwave-IR data calibrated with rain gauges over land. Gridded near-surface wind information (zonal and meridional components -U, V- and intensity UV) was retrieved from the Cross-Calibrated Multi-Platform wind vector analysis (CCMP) version 2, fitting radiometer and scatterometer data, in-situ observations, and ERA-Interim reanalysis into a 6-hourly, 0.25-degree resolution dataset (Wentz et al., 2015). Pointwise observations were retrived with hourly frequency from 312 NOAA stations (NOAA, 2024) for sea-level pressure, near-surface temperature, and wind velocity, and from the Acqua Alta oceanographic tower (AA, 12°30.55′, 45°18.8′, see Figure 1a) for wind velocity.

Sea level information was provided by tide gauge (TG) datasets from 11 stations along the Adriatic coast (3). The original time series consist of hourly sea level elevations. The data of Ancona, Marina di Ravenna, Vieste and Otranto come from ISPRA, Rome (Italian Institute for Environmental Protection and Research; https://www.mareografico.it); Venice data come from CPSM, Venice (Tide Monitoring and Forecast Centre; https://www.comune.venezia.it/node/6214); Trieste data come from CNR-ISMAR, Trieste (Raicich, 2023a, b); Bakar data come from the University of Zagreb (Medugorac et al., 2022, 2023) the data of Rovinj, Zadar, Split, and Dubrovnik come from HHI, Split (Croatian Hydrographic Institute). Sea levels at Rovinj, Bakar, Zadar, Split and Dubrovnik tide gauges were obtained by the mechanical instruments located in a stilling well, with 7-day charts digitized with the Auto-CAD software to obtain hourly sea level values.

Daily sea surface temperature (SST) observations at 0.0417° resolution have been retrieved from the L4 Optimal Interpolation (L4OI) Mediterranean Advanced Very High Resolution Radiometer (AVHRR) SST Analysis dataset (Pisano et al., 2016). A continuous multi-decadal time series for daily in-situ sea water temperature at 2-metre depth on the Trieste harbour station (T2TS, 13°45′ E, 45°39′) was adopted from Raicich and Colucci (2019). The observational reference for basin-wide characterisation of the thermohaline properties of the water masses was given by the CTD profile collection from different survey campaigns described by Pranić et al. (2021) and partially available at https://zenodo.org/record/5707773#.YmkprdpBxPY (Vilibić, 2021).

Due to the absence of the Ionian Sea dynamics in the model implementation and the consequent impossibility of properly reproducing the BiOS signal, the analysis of the sea level variability cannot replicate the approach by Pranić et al. (2021). Likewise, the absence of a very high resolution along the Croatian coast prevents the possibility of relying on the ADCP dataset used in that work for the validation of modelled circulation. Therefore, the scope of the assessment of these quantities in the present work is to verify that the dynamical properties of the basin are compatible with the observations and with the well-known basin-scale circulation features.

The projection of oceanographic processes within a relatively small regional basin and in changing climate conditions is subject to different sources of uncertainty and different levels, from the very evolution of the global climate to how this signal propagates through different scales and how the adopted numerical description impacts the final picture. Extensively tackling all the possible sources of error requires the combination of different techniques and in principle an enormous effort, but the main elements of uncertainty can still be circumscribed at an affordable cost. First, evaluating the performance of the RCM-ROMS modelling chain by pursuing the “perfect boundary conditions” (Christensen et al., 1997) approach driving the RCM with a reanalysis allows to depurate the assessment from the intrinsic errors of the driving GCM. Nonetheless, since this kind of information is obviously not available for the future, the result of this operation is not automatically telling of the capability of the whole modelling chain (GCM-RCM-ROMS in this case) to actually reproduce the future climate. This aspect can be addressed by comparing modelled and observed statistics in the control (CTR, 1987-2016) period providing an aggregated description of the climate variability, under the assumption that the skills exhibited by a climate modelling system under reconstructed radiative forcings (as this is what ultimately drives GCMs in historical simulations) are representative of what can be obtained under projected conditions. Finally, the use of an ensemble approach can provide some degree of information about the uncertainty associated with different modelling strategies. The results of the evaluation (EV) run and of the atmospheric fields used as a forcing under “perfect boundary conditions” are presented and discussed in Section 3.1, whereas the overall climate model skills and uncertainty are addressed in Section 3.2.

Table 3. Tide gauges from the TG dataset and their position in the model grid.

Name	symbol	lat, lon (real)	lat, lon (mod)
Trieste	TS	13.7595, 45.6473	13.7518, 45.6566
Venice Punta Salute	VE	12.3367, 45.4307	12.3451, 45.4206
Bakar	BK	14.5333, 45.3000	14.5080, 45.2819
Rovinj	RO	13.6283, 45.0833	13.6102, 45.0621
Marina di Ravenna	RA	12.2829, 44.4921	12.2957, 44.5104
Zadar	ZD	15.235, 44.1233	15.2330, 44.1480
Ancona	AN	13.5065, 43.6248	13.4885, 43.6443
Split Gradska Luka	SP	16.4417, 43.5067	16.4227, 43.4834
Dubrovnik	DU	18.0633, 42.6583	18.0514, 42.6154
Vieste	VI	16.1770, 41.8881	16.1748, 41.9019
Otranto	OT	18.4971, 40.1472	18.5272, 40.1375

3 Results and discussion

3.1 Evaluation

3.1.1 Atmospheric forcings

An overview of the skills of SMHI-RC4A forced by ERA-INTERIM reanalysis is given in Figure 2. Rainfall and wind appear as the most challenging variables to be properly reproduced, reflecting a recurrent behaviour in RCMs. Strongly spatially and temporally variable quantities like precipitation are intrinsically subject to large errors (Ban et al., 2021; Sangelantoni et al., 2023), and the basin orography and its effect on the land-sea-atmosphere interaction can add a strong element of complexity in the description of the process. Orographic control and the description of the land-sea transition are also a challenging element for the correct reproduction of wind fields, particularly in the Adriatic Sea (Sanchez-Arcilla et al., 2021; Bellafiore et al., 2012; Signell et al., 2005). Furthermore, although being the only available option the evaluation of SMHI-RCA4, ERA-INTERIM known to be far from the “perfect boundary conditions” hypothesis, particularly in terms of rainfall-related quantities (Bao and Zhang, 2013). In turn, slow varying variables as sea-level pressure and near-surface temperature appear well reproduced also at the local scale.

Considering the spatial pattern of the mismatch between model and gridded datasets (Figure 3), the error on daily rainfall is on average mostly within ±2 mm, with a positive bias over the Apennines and western Balkan ridges and a negative bias over the sea. The largest discrepancies (1 and 99 percentile) are mostly encompassed within ±20 mm d^{-1} but can also concern the description of heavier precipitation events, possibly by more than 40 mm d^{-1} on the southern Apennines and along the eastern coast and its mountain ridge. The bias on sea level pressure is within ±3 hPa in most of the domain, with a larger negative value in the southeastern part of the domain. A similar pattern can be found for 1 and 99 percentiles, with a minimum occurring in the same region as the only feature of an otherwise nearly uniform distribution. The near-surface temperature bias over land is negative (up to -3°C in mountain regions) throughout most of the domain, with smaller positive values in the northern coastal areas and in the far northeastern part of the mainland. Extreme values of the difference between model and observations are mostly bracketed in the ±10°C interval, with possible underestimates by more than -12°C in the inner mountain areas.

A separate consideration should be dedicated to the comparison between modelled and observed wind fields. Alongside with the documented tendency of CCMP to globally underestimate relatively strong ($>$15 m s^{-1}, see Mears et al. 2022) wind speed), the quality of this dataset in the Adriatic Sea is hampered by the resolution of the first-guess data source (ERA-INTERIM) and by the largely coastal setting of the basin, in which the use of satellite data for wind estimation is particularly challenging. To partially overcome this limitation, at least in the Northern Adriatic Sea, modelled winds are simultaneously compared with gridded CCMP data and in-situ observations at the Acqua Alta tower. Figure 4 thus shows a generally satisfactory model performance in reproducing the directional distribution of the wind regime, with particular reference to the dominance of northeasterly winds, although slightly overestimating the frequency of moderate to strong winds. In the meantime, while it is confirmed that CCMP underestimates the strong wind events, the directional distribution suffers from a severe overestimate of the frequency of northerly and southwesterly wind, recalling the importance of adopting a specially critical approach when using this dataset for applications in this region.

The statistics displayed in Figure 3 are generally consistent, in terms of range and some features of the spatial patterns (e.g. minimum 1-percentile precipitation difference along the eastern coast, systematic SLP underestimation in the southeast) with those found by Denamiel et al. (2021a). Together with the skill metrics summarised in Figure 2, suggests that the quality of the atmospheric forcings used in the present study should not undergo major shortcomings with respect to a state-of-the-art kilometre-scale implementation, thus performing significantly better than most of the RCMs available for this geographical area in EURO-CORDEX (Kotlarski et al., 2014).

3.1.2 Sea level variability and circulation patterns

The evaluation of the model skills in terms of capability of reproducing sea level variability and hydrodynamics in this study follows a different approach from the analysis carried out by Pranić et al. (2021). In that work, sea level validation was mostly focused on the analysis of spatial EOF components and highlighted a relevant importance of the BiOS signal, which in the present study cannot be properly captured due to the exclusion of the Ionian Sea. In addition, most of the ADCP data used by Pranić et al. (2021) were available along the Croatian coast, where the model resolution can hardly be adequate to reproduce circulation features largely controlled by local, and possibly complex, geometrical and bathymetric constraints.

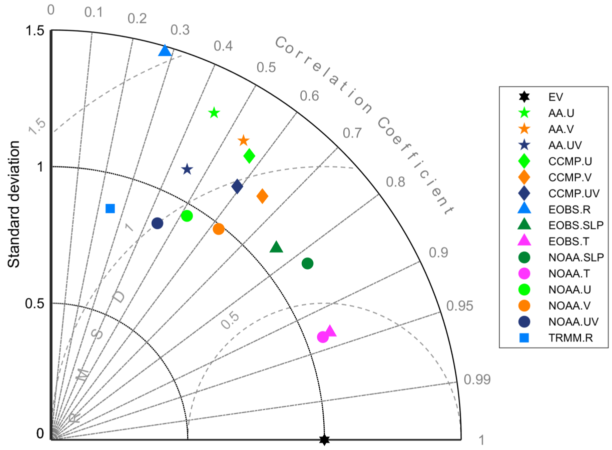

Figure 2. Taylor diagram summarising the normalised skills of the atmospheric forcings used in the evaluation run (EV) compared against the Acqua Alta (AA), CCMP, EOBS, NOAA and TRMM datasets.

These considerations led to the choice of focusing instead on the pointwise comparison of modelled time series against tide gauge records and on the overall features of basin-scale circulation.

Figure 5 presents the scatterplots of observed and modelled daily-averaged sea surface elevation data at 11 stations distributed along both sides, and at different latitudes, of the Adriatic coast. Worth recalling, all time series are depurated from the linear trend and, in the case of observations, from the Sa and SSa tidal components. Although the model undergoes a systematic tendency to underestimate sea level variability within the basin, this limitation seems to progressively reduce for increasing latitudes, namely, for increasing distance from the southern open boundary condition. This northbound improvement of the model skills suggests that internal dynamics partially compensate for the missing variability component in the boundary conditions. Although the use of the present dataset for studies on sea level and its implications (e.g. coastal flooding) at the basin scale should probably require special attention (and most likely an intensive bias adjustment), the fairly good performance on the Northern Adriatic coast permits a more straightforward use in this region, also in terms of boundary conditions for local applications.

The average modelled near-surface circulation at the basin scale (a) and in the northermost region (b) is presented in Figure 6. Although the time-averaging smooths out the seasonal variability, the model appears capable to reproduce the main well-known patterns (Lipizer et al. 2014 and references therein; Cushman-Roisin et al. 2001). Along the Eastern coast the inflowing Eastern Adriatic Current is well visible alongside with its cyclonic recirculations around the Southern Adriatic Pit (Southern Adriatic Gyre), the Jabuka Pit (Mid Adriatic Gyre), and the northern coast (Northern Adriatic Gyre), whereas the Western Adriatic Current flows southbound along the Italian coast. In the northern Adriatic, the signature of the typically wintry gyre encompassed between the Po Delta and the Istrian Peninsula (that is, north of 45°N) is partially visible also from the multi-

https://doi.org/10.5194/egusphere-2024-1468
Preprint. Discussion started: 30 May 2024

decadal, year-round averaging, together with the cyclonic structure recirculating water masses from the northern Dalmatian islands to the Italian coast between the Po Delta and Ancona (43°36′ to 45°N, see Carniel et al. 2016).

3.1.3 Thermohaline properties

The assessment of the model skills in reproducing the thermohaline properties of the Adriatic sea, as well as their variability over multiple time scales, is crucial for investigating its usability and possible limitations for a broad set of applications. Sea surface temperature (SST) is not only a key variable for the characterisation of air-sea heat fluxes and the numerical modelling description of possibly intense meteo-oceanic events such as tropical-like cyclones and heavy precipitation events (Ricchi et al., 2017, 2021), but is also a reference parameter for the identification of extreme events such as Cold Spells (CS) and Marine Heat Waves (MHWs), for which one of the most broadly accepted definition (Hobday et al., 2016) is based on the persistence respectively below the climatological 10th percentile or above the climatological 90th percentile for a period longer than 5 days. The difference between modelled (EV run) and observed (AVHRR) seasonal values for 10th, 50th and 90th percentiles are shown in Figure 7.

Overall, modelled SST statistics are generally characterised by relatively small errors, mostly bracketed in ± 1 °C and spatially distributed in patchy and mostly uncoherent structures. In winter (December to February), a cold bias affects the coastal regions of the western and south-eastern Adriatic, with an underestimate mostly smaller than -1 °C but particularly marked (exceeding -2 °C) for 10th percentile along the central Italian coast. In the same season, SST seems overestimated in the open sea and in some segments of the northern and southwestern coast in a range between less than 0.5 °C (10th percentile) and 1.5 °C (90th percentile). In spring (March to May) the picture in the north appears reversed with a moderate overestimate ($<$ 1 °C) of 10th and 50th percentile SST and an underestimate (locally up to -1.5 °C off the Po delta) of the warmer conditions (90th percentile), though with the persistence of a small (generally $<$ 0.5 °C) warm bias in the central and southern regions and a small cold bias along the southeastern coast. Summer (June to August) SST appear mostly subject to a variable degree of underestimate, more marked (locally exceeding -1 °C) in most of the northern and central regions and along the southeastern coast, with a notable exception in the Kvarner Bay where a persistent positive bias (approximately 1 °C) occurs. In turn, modelled autumn (September to November) values appear generally overestimated in most of the basin, with a maximum exceeding 1.5 °C off the Po delta. In aggregated terms (Figure 8), the mismatch between modelled and observed SST values lies in the ± 3 °C (respectively 1st and 99th percentile of the model-observations difference) in most of the basin, with larger absolute values (locally up to ± 4 °C) off the Po delta and, for 1st percentile, along the central Italian coast. This range is similar to the one discussed by Pranić et al. (2021) with reference to the AdriSC model, although the pattern in that work exhibited a more pronounced zonal gradient, with lower temperatures (that is, larger negative and smaller positive errors) along the western coast. Worth noting, also the modelled warming trends in the period (Figure 9), ranging between 0.25 and 0.40 °C per decade, are consistent with previous estimates (Mohamed et al., 2019; Amos et al., 2017; Tojčić et al., 2023) based on different observational datasets and slightly different time periods, suggesting that SST does not show any macroscopic sign of a spurious drift related to the model implementation.

https://doi.org/10.5194/egusphere-2024-1468
Preprint. Discussion started: 30 May 2024

The analysis of the model results against the complete available three-dimensional thermohaline information can provide, alongside with a deeper insight on the model capability to capture the basin dynamics, a key for the interpretation of the SST-based skill assessment. In this direction, a first broad overview is given by Taylor diagrams and quantile-quantile plots referred to the CTD dataset in the subdomains and in the whole Adriatic Sea (Figure 10). Model skills in terms of potential temperature (θ) appear generally better, and less variable among subdomains, than in terms of salinity (S). Overall, intermediate values of $theta$ tend to be overestimated by the model, particularly in the Northern Adriatic subdomain, whereas the tails of the potential temperature distribution are generally well reproduced in all subdomains. In turn, while intermediate to high S values are mostly well reproduced, low to mid salinity tends to be overestimated, particularly in the Kvarner Bay and in the Dalmatian Islands. Like in the case of SST, also skills for 3D θ and S are comparable with the values found for AdriSC by Pranić et al. (2021), although the metrics discussed in that work consider all the subdomains aggregately while distinguishing among different campaign datasets. In terms of potential density anomaly (σ_θ), intermediate values are generally underestimated (in the Northern Adriatic, which is the most unfavourable situation, up to approximately 0.6 kg m^{-3}), but for higher values the performance tends to improve, with the mismatch progressively decreasing to less than 0.2 kg m^{-3} for σ_θ greater than 29.4 kg m^{-3}. Importantly, Taylor diagrams also show a very small influence of the version of the CMEMS product used for the boundary conditions on the overall statistic. This suggests that the climate ensemble, whose implementation began before the release of the latest version of MFS (Escudier et al., 2020), should not be considered prone to major elements of obsolescence associated with the use of a previous dataset (Simoncelli et al., 2019). Although again aggregated at the subdomain scale, Figure 11 shows how model errors are distributed over time and along the water column. Here we focus on the Northern Adriatic (panels a and d), Kvarner Bay (b and e) and Deep Adriatic (c and f) due to the relevance of these areas for dense water dynamics and the contribution of the Adriatic Sea for the Mediterranean thermohaline circulation.

In the Northern Adriatic, θ medians exhibit a very close match between model and observations during the winter months, while the temperature overestimate progressively increases in spring and summer, and mostly below the 15-metre depth, likely as an effect of excess of vertical mixing. Such a heat content surplus is then redistributed throughout the water column in autumn and progressively reduced to very small values. The seasonal variability is not as clear for S in this region, but in this case the vertical distribution of the error reaches its maximum values close to the surface, possibly reverberating the uncertainty in the description of freshwater inputs and its implications for plume dynamics. The performance in terms of σ_θ appears mostly controlled by temperature values, with larger errors for higher depths and better agreement in winter and close to the surface. In the Kvarner Bay the overestimate in summer temperature, with a similar profile as in the Northern Adriatic, is particularly evident compared with the other seasons, while S remains slightly overestimated throughout the whole year, with larger errors concentrated in the upper 10 metres. In this case, near-surface σ_θ errors appear mostly controlled by salinity, particularly in spring and summer, whereas θ errors control the winter profile of the error and the sub-surface part of the summer profile. In the deep Adriatic, an apparent tendency to underestimate average values of θ and S throughout the year is actually the result of some shortcomings in the description of thermohaline properties in the upper layers. The θ overestimate in the sub-surface layer (approximately for between 10 and 100 m depth) reported in summer and autumn reflects the patterns observed in the northern regions, and is consistent with a possible excess in vertical mixing. The same explanation can be proposed for the overestimate in the near-surface S values in the same months, whereas some systematic, though relatively small (approximately around -1) underestimate at intermediate depth (100 - 400 m) appears possibly due with some bias in the boundary conditions. Error values are definitely smaller in the deeper layer, which is the one where deep ventilation occurs and whose σ_θ background values exert a fundamental control in dense shelf water downflow.

3.1.4 Extreme thermal events

Extreme events are typically an element of major interest in climate projections. With specific reference to thermal extremes, besides the well-acknowledged role of wintry cold air outbreaks in dense water formation in the Adriatic Sea, there is increasing awareness of the potential effect of Marine Heat Waves (MHWs) and Cold Spells on marine systems, with particular concern with the impacts on coastal and transitional environments (see Ferrarin et al. 2023, and references therein). In this perspective, a separate section of the evaluation is dedicated to the assessment of the EV run to capture the key features of observed extreme events. MHW (CS) are identified following Hobday et al. (2016), as periods longer than 5 days in which sea surface temperature is persistently above (below) the daily climatological 90th (10th) percentile in the reference period (an 11-day sliding window was considered in this application), while the cumulative intensity is defined as the difference between current value and climatological daily mean integrated over the event duration. Focusing on the in-situ records collected at Trieste, Figure 12 shows that timing (panel c) and intensity (panel d) of these events are generally well reproduced. In particular, the modelling chain seems to satisfactorily capture most of the features of the interannual variability and the alternation of ordinary periods (e.g. 1995-1998) and exceptional years (e.g. 1987, 2001, 2007), although with some remarkable exceptions such as in 2006. The intra-annual variability of the occurrence of thermal extremes appears also at least partially well captured, with some increase in MHW occurrence in summer (worth recalling, this is not obvious, as the definition of these events in different periods throughout the year is referred to the statistics of the same period) occurring also in the EV results (panel e), while some shortcomings appear in the reproduction of the very weak modulation of CS occurrence (panel f).

3.2 Climate runs: overview

If the focus on the EV run allows to investigate the model skills in the presence of the better available, if not actually “perfect”, information, the analysis of the climate ensemble allows investigate the model capability to reproduce the observed climate statistics in the recent past, besides obviously the possible variations in the future scenario (SCE, 2070-2099), and the uncertainty associated with the use of different GCMs. Again with reference to the three subdomains considered in Figure 11, the climate normals of the monthly values of 1st, 50th and 99th percentile of SST in different data sets are shown in Figure 13. As a recurring pattern, the climate ensemble statistics appear satisfactorily matching the observations in the winter months, while underestimating and overestimating respectively summer and autumn values, most likely as a result of the description of the fluxes of heat along the upper layers of the water column associated with the excess mixing described in Section 3.1. This behaviour is more evident in the Northern Adriatic, where the maximum mismatch reaches 2.7 °C for the 99th percentile in June. The ensemble spread is generally narrow (around 1 °C) from October to April both in CTR and SCE conditions, and significantly larger (> 4 °C) in summer, particularly in the SCE datasets, in some cases obscuring the statistical significance

https://doi.org/10.5194/egusphere-2024-1468
Preprint. Discussion started: 30 May 2024

of the future change signal. An examination of uncertainty partitioning through the different modelling chain steps lies beyond the scope of the present study, however, speculations can be made about the well-known large uncertainty charactering GCMs in reproducing crucial mid-latitude summer season dynamics like blocking atmospheric patterns (Davini and D'Andrea, 2020) and their response to a warmer climate (Woollings, 2010; Woollings et al., 2018). Nevertheless, also a local scale forcing can be expected behind resulting ensemble variability and exerted by the nested simulations (SMHI-RCA4 and ROMS) given the non-linear ingestion of the GCM large-scale signal. The SST increase between SCE and CTR is generally evenly distributed throughout the year and among the different statistics, ranging in most cases, for ensemble means, between +2.8 and +3.2 °C.

A broader view on how climate change affects the statistics of the thermohaline properties of the Adriatic Sea (and of the subdomains considered in this study) can be drawn from the quantile-quantile plots depicted in Figure 14.

While the projected potential temperature increase in the colder (and deeper) regions of the deep Adriatic is confined below 1.5 °C, the statistics throughout the different basins reflect the pattern presented in Figure 13, with variations mostly clustered around +3 °C. Projected ensemble average salinity increase is mostly encompassed between 0.3 and 0.4, with larger variations on the higher end of the distribution (namely, for $S \geq 39$). In terms of σ_{theta} variations, this results in a generalised tendency towards a decrease between 0.4 and 0.5 kg m^{-3} in most of the basin (with the larger decrease corresponding to smaller values), with the exception of the deeper regions of the deep Adriatic, presently characterised by σ_θ around 29.2 kg m^{-3} facing a decrease of approximately 0.2 kg m^{-3}. Most notably, Figure 14 shows that the variability of the results within the ensemble is generally larger than the variability across the subdomains: since the evidences from the EV run (Section 3.1) support a good degree of confidence in the model capability of reproducing the internal dynamics of the Adriatic Sea, this result gives an important account of the relative weight of the GCM-RCM modelling chain in the ocean climate projections at the basin scale.

Figure 15 summarises the seasonal modulation of the variation of thermohaline (median) quantities along the water column, again with a focus on the relevant basins for dense water formation and deep ventilation. NA and KB are characterised by similar results, in both qualitative and quantitative terms. In NA (KB), the ensemble-mean increase in median θ values ranges between +2.5 (+2.6) and +2.7 (+2.8) °C in winter and spring, and between +2.9 (+2.9) and +3.1 (+3.2) °C in summer, with intermediate variations between +2.7 and +2.8 (+2.8, nearly uniform) °C in autumn. S exhibits a more pronounced vertical variability. For depth smaller than 40 m, increases range between +0.28 (+0.37) in winter and +0.71 (+0.49) in summer, whereas for higher depths the range of the increase lies between +0.34 and +0.43 (+0.32 and +0.43). Median σ_θ is thus projected to decrease by -0.27 (-0.29) kg m^{-3} in winter, when dense water formation typically takes place, and between -0.27 (-0.36) and -0.42 (-0.40) kg m^{-3}, with the largest values for depths larger than 40 m, in autumn. Variations in spring and summer, respectively in the range -0.34 (-0.36) to -0.32 (-0.34) and -0.55 (-0.57) to -0.41 (-0.46) kg m^{-3}, although with relevant values, are less significant for the thermohaline circulation in the basin. In DA, the seasonal modulation of climate change on median profiles is mostly visible for $h le 200$ m; for larger depths, thermohaline quantities vary gradually, and with negligible inter-seasonal differences, up to uniform values for $h \geq 800$ m. In the upper layer, variations range between +2.5 and +3.2 °C for θ and between +0.26 and +0.37 for S, again with smaller variations in winter and spring and larger variations in summer and autumn. σ_θ variations range between -0.40 kg m^{-3} in spring and -0.71 kg m^{-3} in summer. Below the upper layer, θ increase

https://doi.org/10.5194/egusphere-2024-1468
Preprint. Discussion started: 30 May 2024

varies from + 2.8°C for h=200 m to +1.3°C for h$\geq$800 m, S increase varies from +0.21 to +0.17, and σ_θ varies between -0.44 and -0.15 kg m^{-3}.

Before focusing on thermal extremes such as MHWs and CSs, it is worth recalling that the definition of these events (Hobday et al., 2016) is intrinsically associated with some definition of impact, in most cases in the framework of the discourse on climate change. In this direction, the choice of the baseline period as a reference for the computation of the threshold percentiles implies an important assumption on the system on which MHWs and CSs are supposed to act as stressors. More precisely, defining these events in a future scenario with reference to a past climatology implicitly assumes that the target system has not undergone significant changes over time; in turn, defining these events with reference to a future climatology is compatible with the assumption that the system has adapted to the change in the “ordinary” conditions and is only (or mostly) vulnerable to significant deviations to those conditions. In the present study, taking as reference thresholds climatological values from the CTR period yields the simple, though important, result that end-of-century conditions under RCP8.5 climate scenario are persistently corresponding to MHW. For this reason, this hypothesis is not considered in the plots in Figure 16, in which MHWs and CSs are defined for CTR and SCE, as well as for the EV run and for observations in the control period, with reference to the climatologies for the corresponding periods. Under this approach, modelled differences between SCE and CTR conditions (expressed as monthly mean cumulative intensity of the events) appear generally minor and in any case only occasionally statistically significant. If true, this would suggest that climate change impacts on ecosystems could be mainly controlled by the warming trend of the ordinary conditions, with only a secondary contribution from the change in the extremes of the thermal statistical distribution. Nonetheless, it is worth noting that the RCM-ROMS modelling chain exhibits some shortcomings in properly capturing the cumulative intensity of extreme events between late spring and early summer (mostly in May and June). While the mismatch is generally fairly small in the case of the EV run (although with the caveat that the reference period is slightly different), this is more evident in the case of the CTR run, thus revealing, alongside with the limitations already pointed out in the model performance (e.g. the excess in vertical mixing), some limitations in the GCM-RCM capability to reproduce the extremes during the warm season.

4 Conclusions

The present paper introduces a six-member kilometre-scale ocean model ensemble tackling end-of-century changes in the dynamics of the Adriatic Sea under a RCP8.5 climate scenario. Up to our best knowledge, this is the first effort undertaken to characterise the effects of climate change on ocean dynamics in this region by combining the detail of the high resolution and a measure of the uncertainty as provided by the ensemble approach. The aim of this work is to pave the way for an extensive variety of multidisciplinary studies related to climate impacts on the Adriatic Sea, ranging from the possible changes in deep sea ventilation regimes to the dynamics and evolution of marine habitats, also including downscaling for local applications in coastal and transitional systems. In this direction, special attention was dedicated to a thorough assessment of the model skills, whereas the climate projections have been introduced in terms of expected variation and uncertainty on thermohaline quantities, with a focus on extreme thermal events. The set of processes and statistics addressed in the validation is meant to provide an overview on the applicability and limitations of the model ensemble to a broad variety of applications. The resolution of the atmospheric model (0.11 deg) might be too coarse to properly reproduce extreme events, like the bora wind, bora-driven ocean circulation and formation of dense water (Kuzmić et al., 2015; Denamiel et al., 2021b; Pranić et al., 2023). This particularly applies to the complex coastal basin of the Kvarner Bay over which the bora-driven heat uptake reaches its maximum (Janeković et al., 2014) and which is recently assessed to contribute about 25-35% to the overall dense waters (Mihanović et al., 2018). Also, the cascading of dense waters in the Southern Adriatic Pit might be underestimated, as the model resolution in this area is probably too coarse to properly capture submarine canyons in which the dense waters are known to cascade (e.g., Paladini de Mendoza et al. 2022). Further, AdriE ensemble models have no capacity to address BiOS-driven quasi-decadal variability in thermohaline properties of the Adriatic, as requiring the inclusion of the northern Ionian Sea (in which the BiOS-driven circulation regimes) into the domain (Denamiel et al., 2022). Nonetheless, and the comparison against the previous work by Pranić et al. (2021), purportedly carried out for the evaluation run wherever possible, shows that the performance of the SMHI-RCA4 - ROMS modelling chain is mostly aligned with the skills of a state-of-the-art kilometre-scale hindcast, in particular over the northern Adriatic in which resolution of the ocean model is at the kilometre-scale (ca. 2 km). In any case, for studies focused on specific processes (e.g. plume dynamics, lagrangian transport, fluxes across the continental margin) a specific validation is strongly recommended. In this paper the general scope of the dataset led to the decision to focus the discussion on the raw model outputs, while the possible bias adjustment strategies should be decided from time to time for each specific application based on its characteristics and on the trade-offs involved (Enayati et al., 2021).

Concerning the climate projections, the main results presented in this work can be summarised as follows:

- in ensemble-average terms, end-of-century projected SST increase is encompassed between +2.8 °C and +3.2 °C, with an uncertainty range of approximately 1 °C and in winter and up to 4 °C in summer;

- in general, the variation in thermohaline quantities is also larger, in absolute terms, in summer and autumn and smaller in winter and spring;

- over the considered time span, the variability of the change in thermohaline quantities within the ensemble is larger than across the subdomains, suggesting that any additional detail in the long-term projection deriving from a kilometre-scale approach could be curbed by the uncertainty in the regional and global climate evolution, if these are not properly taken into account;

- with reference to the recent past statistics, future conditions could be assimilated to a massive, persistent MHW; conversely, taking as reference the future “ordinary” conditions (that is, implicitly assuming that the target system, however defined in socio-ecological terms, has adapted to the new state), the model ensemble does not provide strong evidences of major variations in the statistics of the thermal extremes. Worth noting, the observed shortcomings in the climate modelling chain capability to reproduce thermal extremes in summer suggest that this result should be taken with special care.

Monthly-averaged fields for the main oceanographic quantities from the climate simulations, as well as fields from the EV run, are publicly available on Zenodo (Bonaldo et al., 2024), whereas specific requests for other variables or time resolution can be submitted to the corresponding author.

Data availability. Monthly averages of the main quantities are available on Zenodo (https://zenodo.org/records/11202265), and subsets of the full modelling dataset can be requested to the corresponding author.

Author contributions. DB coordinated the study and the preparation of the manuscript, DB, AR, and LS set up the model runs, DB, CD, PP, FR, AR, LS, and IV contributed in the model validation and analysis, all authors participated in the discussion of the results and in the editing of the text.

Competing interests. The authors have no competing interests to be declared

Acknowledgements. We acknowledge the E-OBS dataset from the EU-FP6 project UERRA (https://www.uerra.eu) and the Copernicus Climate Change Service, and the data providers in the ECA&D project (https://www.ecad.eu). The contribution of all the organizations that provided the CTD observational data used in this study is also gratefully acknowledged.

References

Amos, C. L., Umgiesser, G., Ghezzo, M., Kassem, H., and Ferrarin, C.: Sea Surface Temperature Trends in Venice Lagoon and the Adjacent Waters, Journal of Coastal Research, 33, 385 – 395, https://doi.org/10.2112/JCOASTRES-D-16-00017.1, 2017.

Ban, N., Caillaud, C., Coppola, E., Pichelli, E., Sobolowski, S., Adinolfi, M., Ahrens, B., Alias, A., Anders, I., Bastin, S., Belušić, D., Berthou, S., Brisson, E., Cardoso, R. M., Chan, S. C., Christensen, O. B., Fernández, J., Fita, L., Frisius, T., Gašparac, G., Giorgi, F., Goergen, K., Haugen, J. E., Øivind Hodnebrog, Kartsios, S., Katragkou, E., Kendon, E. J., Keuler, K., Lavin-Gullon, A., Lenderink, G., Leutwyler, D., Lorenz, T., Maraun, D., Mercogliano, P., Milovac, J., Panitz, H. J., Raffa, M., Remedio, A. R., Schär, C., Soares, P. M., Srnec, L., Steensen, B. M., Stocchi, P., Tölle, M. H., Truhetz, H., Vergara-Temprado, J., de Vries, H., Warrach-Sagi, K., Wulfmeyer, V., and Zander, M. J.: The first multi-model ensemble of regional climate simulations at kilometer-scale resolution, part I: evaluation of precipitation, Climate Dynamics, 57, 275–302, https://doi.org/10.1007/s00382-021-05708-w, 2021.

Bao, X. and Zhang, F.: Evaluation of NCEP–CFSR, NCEP–NCAR, ERA-Interim, and ERA-40 Reanalysis Datasets against Independent Sounding Observations over the Tibetan Plateau, Journal of Climate, 26, 206 – 214, https://doi.org/10.1175/JCLI-D-12-00056.1, 2013.

Bargain, A., Foglini, F., Pairaud, I., Bonaldo, D., Carniel, S., Angeletti, L., Taviani, M., Rochette, S., and Fabri, M.: Predictive habitat modeling in two Mediterranean canyons including hydrodynamic variables, Progress in Oceanography, pp. 0–1, https://doi.org/10.1016/j.pocean.2018.02.015, 2018.

Bellafiore, D., Bucchignani, E., Gualdi, S., Carniel, S., Djurdjević, V., and Umgiesser, G.: Assessment of meteorological climate models as inputs for coastal studies, Ocean Dynamics, 62, 555–568, https://doi.org/10.1007/s10236-011-0508-2, 2012.

Benetazzo, A., Fedele, F., Carniel, S., Ricchi, A., Bucchignani, E., and Sclavo, M.: Wave climate of the Adriatic Sea: A future scenario simulation, Natural Hazards and Earth System Science, 12, 2065–2076, https://doi.org/10.5194/nhess-12-2065-2012, 2012.

Benetazzo, A., Bergamasco, A., Bonaldo, D., Falcieri, F., Sclavo, M., Langone, L., and Carniel, S.: Response of the Adriatic Sea to an intense cold air outbreak: Dense water dynamics and wave-induced transport, Progress in Oceanography, 128, 115–138, https://doi.org/10.1016/j.pocean.2014.08.015, 2014.

Bergamasco, A. and Malanotte-Rizzoli, P.: The circulation of the Mediterranean Sea: a historical review of experimental investigations, Advances in Oceanography and Limnology, 1, 11–28, https://doi.org/10.1080/19475721.2010.491656, 2010.

Bonaldo, D., Benetazzo, A., Bergamasco, A., Campiani, E., Foglini, F., Sclavo, M., Trincardi, F., and Carniel, S.: Interactions among Adriatic continental margin morphology, deep circulation and bedform patterns, Marine Geology, 375, 82–98, https://doi.org/10.1016/j.margeo.2015.09.012, 2016.

Bonaldo, D., Antonioli, F., Archetti, R., Bezzi, A., Correggiari, A., Davolio, S., Falco, G. D., and Fantini, M.: Integrating multidisciplinary instruments for assessing coastal vulnerability to erosion and sea level rise: lessons and challenges from the Adriatic Sea , Italy, Journal of Coastal Conservation, 23, 19–37, 2019.

Bonaldo, D., Bucchignani, E., Pomaro, A., Ricchi, A., Sclavo, M., and Carniel, S.: Wind waves in the Adriatic Sea under a severe climate change scenario and implications for the coasts, International Journal of Climatology, 40, 5389–5406, https://doi.org/10.1002/joc.6524, 2020.

Bonaldo, D., Carniel, S., Colucci, R. R., Denamiel, C., Pranić, P., Raicich, F., Ricchi, A., Sangelantoni, L., Vilibić, I., and Vitelletti, M. L.: AdriE ocean climate model ensemble for the Adriatic Sea - monthly fields [Data set], https://doi.org/10.5281/zenodo.11202265, 2024.

Carniel, S., Benetazzo, A., Bonaldo, D., Falcieri, F., Miglietta, M., Ricchi, A., and Sclavo, M.: Scratching beneath the surface while coupling atmosphere, ocean and waves: Analysis of a dense water formation event, Ocean Modelling, 101, https://doi.org/10.1016/j.ocemod.2016.03.007, 2016.

Christensen, J. H., Machenhauer, B., Jones, R. G., Scha¨r, C. S., Ruti, P. M., Castro, M., and Visconti, G.: Climate Dynamics Validation of present-day regional climate simulations over Europe: LAM simulations with observed boundary conditions, 1997.

Christensen, O. B. and Kjellström, E.: Partitioning uncertainty components of mean climate and climate change in a large ensemble of European regional climate model projections, Climate Dynamics, 54, 4293–4308, https://doi.org/10.1007/s00382-020-05229-y, 2020.

Christensen, O. B. and Kjellström, E.: Filling the matrix: an ANOVA-based method to emulate regional climate model simulations for equally-weighted properties of ensembles of opportunity, Climate Dynamics, 58, 2371–2385, https://doi.org/10.1007/s00382-021-06010-5, 2022.

Church, J., Clark, P., Cazenave, A., Gregory, J., Jevrejeva, S., Levermann, A., Merrifield, M., Milne, G., Nerem, R., Nunn, P., Payne, A., Pfeffer, W., Stammer, D., and Unnikrishnan, A.: Sea Level Change. In: Climate Change 2013: The Physical Science Basis. Contribution of Working Group I to the Fifth Assessment Report of the Intergovernmental Panel on Climate Change, Cambridge University Press, Cambridge, United Kingdom and New York, NY, USA, 2013.

Cornes, R. C., van der Schrier, G., van den Besselaar, E. J. M., and Jones, P. D.: An Ensemble Version of the E-OBS Temperature and Precipitation Data Sets, Journal of Geophysical Research: Atmospheres, 123, 9391–9409, https://doi.org/https://doi.org/10.1029/2017JD028200, 2018.

Cushman-Roisin, B., Gačić, M., Poulain, P., and Artegiani, A.: Physical Oceanography of the Adriatic Sea: past, present and future, Springer - Science+Business Media, B.V., https://doi.org/10.1007/978-94-015-9819-4, 2001.

Davini, P. and D'Andrea, F.: From CMIP3 to CMIP6: Northern Hemisphere Atmospheric Blocking Simulation in Present and Future Climate, Journal of Climate, 33, 10 021 – 10 038, https://doi.org/10.1175/JCLI-D-19-0862.1, 2020.

Dee, D. P., Uppala, S. M., Simmons, A. J., Berrisford, P., Poli, P., Kobayashi, S., Andrae, U., Balmaseda, M. A., Balsamo, G., Bauer, P., Bechtold, P., Beljaars, A. C. M., van de Berg, L., Bidlot, J., Bormann, N., Delsol, C., Dragani, R., Fuentes, M., Geer, A. J., Haimberger, L., Healy, S. B., Hersbach, H., Hólm, E. V., Isaksen, L., Kållberg, P., Köhler, M., Matricardi, M., McNally, A. P., Monge-Sanz, B. M., Morcrette, J.-J., Park, B.-K., Peubey, C., de Rosnay, P., Tavolato, C., Thépaut, J.-N., and Vitart, F.: The ERA-Interim reanalysis: configuration and performance of the data assimilation system, Quarterly Journal of the Royal Meteorological Society, 137, 553–597, https://doi.org/https://doi.org/10.1002/qj.828, 2011.

Denamiel, C., Pranić, P., Quentin, F., Mihanović, H., and Vilibić, I.: Pseudo-global warming projections of extreme wave storms in complex coastal regions: the case of the Adriatic Sea, CLIMATE DYNAMICS, 55, 2483–2509, https://doi.org/10.1007/s00382-020-05397-x, 2020.

Denamiel, C., Pranić, P., Ivanković, D., Tojčić, I., and Vilibić, I.: Performance of the Adriatic Sea and Coast (AdriSC) climate component - a COAWST V3.3-based coupled atmosphere-ocean modelling suite: atmospheric dataset, Geoscientific Model Development, 14, 3995–4017, https://doi.org/10.5194/gmd-14-3995-2021, 2021a.

Denamiel, C., Tojčić, I., and Vilibić, I.: Balancing Accuracy and Efficiency of Atmospheric Models in the Northern Adriatic During Severe Bora Events, Journal of Geophysical Research: Atmospheres, 126, e2020JD033 516, https://doi.org/https://doi.org/10.1029/2020JD033516, e2020JD033516 2020JD033516, 2021b.

Denamiel, C., Tojčić, I., Pranić, P., and Vilibić, I.: Modes of the BiOS - driven Adriatic Sea thermohaline variability, Climate Dynamics, 59, 1097–1113, https://doi.org/10.1007/s00382-022-06178-4, 2022.

https://doi.org/10.5194/egusphere-2024-1468
Preprint. Discussion started: 30 May 2024

Dunić, N., Vilibić, I., Šepić, J., Mihanović, H., Sevault, F., Somot, S., Waldman, R., Nabat, P., Arsouze, T., Pennel, R., Jordà, G., and Precali, R.: Performance of multi-decadal ocean simulations in the Adriatic Sea, Ocean Modelling, 134, 84–109, https://doi.org/10.1016/j.ocemod.2019.01.006, 2019.

Dunić, N., Supić, N., Sevault, F., and Vilibić, I.: The northern Adriatic circulation regimes in the future winter climate, Climate Dynamics, https://doi.org/10.1007/s00382-022-06516-6, 2022.

Egbert, G. D. and Erofeeva, S. Y.: Efficient Inverse Modeling of Barotropic Ocean Tides, Journal of Atmospheric and Oceanic Technology, 19, 183–204, https://doi.org/10.1175/1520-0426(2002)019<0183:EIMOBO>2.0.CO;2, 2002.

Enayati, M., Bozorg-Haddad, O., Bazrafshan, J., Hejabi, S., and Chu, X.: Bias correction capabilities of quantile mapping methods for rainfall and temperature variables, Journal of Water and Climate Change, 12, 401–419, https://doi.org/10.2166/wcc.2020.261, 2021.

Escudier, R., Clementi, E., Omar, M., Cipollone, A., Pistoia, J., J, A., Drudi, M., Grandi, A., Lyubartsev, V., Lecci, R., Cretí, S., Masina, S., Coppini, G., and Pinardi, N.: Mediterranean Sea Physical Reanalysis (CMEMS MED-Currents) (Version 1, Data set).Copernicus Monitoring Environment Marine Service (CMEMS), https://doi.org/10.25423/CMCC/MEDSEA_MULTIYEAR_ PHY_006_004_E3R1, 2020.

Ferrarin, C., Bonaldo, D., Bergamasco, A., and Ghezzo, M.: Sea level and temperature extremes in a regulated Lagoon of Venice, Frontiers in Climate, 5, https://doi.org/10.3389/fclim.2023.1330388, 2023.

Haidvogel, D., Arango, H., Budgell, W., Cornuelle, B., Curchitser, E., Di Lorenzo, E., Fennel, K., Geyer, W., Hermann, A., Lanerolle, L., Levin, J., McWilliams, J., Miller, A., Moore, A., Powell, T., Shchepetkin, A., Sherwood, C., Signell, R., Warner, J., and Wilkin, J.: Ocean forecasting in terrain-following coordinates: Formulation and skill assessment of the Regional Ocean Modeling System, Journal of Computational Physics, 227, 3595–3624, 2008.

Hobday, A. J., Alexander, L. V., Perkins, S. E., Smale, D. A., Straub, S. C., Oliver, E. C., Benthuysen, J. A., Burrows, M. T., Donat, M. G., Feng, M., Holbrook, N. J., Moore, P. J., Scannell, H. A., Gupta, A. S., and Wernberg, T.: A hierarchical approach to defining marine heatwaves, Progress in Oceanography, 141, 227–238, https://doi.org/10.1016/j.pocean.2015.12.014, 2016.

Huffman, G., Bolvin, D., Nelkin, E., and Adler, R.: TRMM (TMPA) Precipitation L3 1 day 0.25 degree x 0.25 degree V7, Edited by Andrey Savtchenko, Goddard Earth Sciences Data and Information Services Center (GES DISC), Accessed: 21 Dec 2023, 10.5067/TRMM/TMPA/DAY/7, https://doi.org/10.5067/TRMM/TMPA/DAY/7, 2016.

Janeković, I., Mihanović, H., Vilibić, I., and Tudor, M.: Extreme cooling and dense water formation estimates in open and coastal regions of the Adriatic Sea during the winter of 2012, Journal of Geophysical Research: Oceans, 119, 3200–3218, https://doi.org/10.1002/2014JC009865, 2014.

Kotlarski, S., Keuler, K., Christensen, O. B., Colette, A., Déqué, M., Gobiet, A., Goergen, K., Jacob, D., Lüthi, D., van Meijgaard, E., Nikulin, G., Schär, C., Teichmann, C., Vautard, R., Warrach-Sagi, K., and Wulfmeyer, V.: Regional climate modeling on European scales: a joint standard evaluation of the EURO-CORDEX RCM ensemble, Geoscientific Model Development, 7, 1297–1333, https://doi.org/10.5194/gmd-7-1297-2014, 2014.

Kuzmić, M., Grisogono, B., Li, X., and Lehner, S.: Examining deep and shallow Adriatic bora events, Quarterly Journal of the Royal Meteorological Society, 141, 3434–3438, https://doi.org/https://doi.org/10.1002/qj.2578, 2015.

Lionello, P., Galati, M. B., and Elvini, E.: Extreme storm surge and wind wave climate scenario simulations at the Venetian littoral, Physics and Chemistry of the Earth, 40-41, 86–92, https://doi.org/10.1016/j.pce.2010.04.001, 2012.

Lipizer, M., Partescano, E., Rabitti, A., Giorgetti, A., and Crise, A.: Qualified temperature, salinity and dissolved oxygen climatologies in a changing Adriatic Sea, Ocean Science, 10, 771–797, https://doi.org/10.5194/os-10-771-2014, 2014.

https://doi.org/10.5194/egusphere-2024-1468
Preprint. Discussion started: 30 May 2024

Mears, C., Lee, T., Ricciardulli, L., Wang, X., and Wentz, F.: Improving the Accuracy of the Cross-Calibrated Multi-Platform (CCMP) Ocean Vector Winds, Remote Sensing, 14, https://doi.org/10.3390/rs14174230, 2022.

Medugorac, I., Pasarić, M., and Orlić, M.: Long-term measurements at Bakar tide-gauge station (east Adriatic), Geofizika, 39, 151–162, https://doi.org/10.15233/gfz.2022.39.8, 2022.

Medugorac, I., Pasarić, M., and Orlić, M.: Historical sea-level measurements at Bakar (east Adriatic), https://doi.org/10.17882/85171, https://www.seanoe.org/data/00740/85171/, 2023.

Mihanović, H., Janeković, I., Vilibić, I., Kovačević, V., and Bensi, M.: Modelling Interannual Changes in Dense Water Formation on the Northern Adriatic Shelf, Pure and Applied Geophysics, 175, 4065–4081, https://doi.org/10.1007/s00024-018-1935-5, 2018.

Mohamed, B., Abdallah, A. M., Alam El-Din, K., Nagy, H., and Shaltout, M.: Inter-Annual Variability and Trends of Sea Level and Sea Surface Temperature in the Mediterranean Sea over the Last 25 Years, Pure and Applied Geophysics, 176, 3787–3810, https://doi.org/10.1007/s00024-019-02156-w, 2019.

Orlić, M., Gacić, M., and La Violette, P. E.: The currents and circulation of the Adriatic Sea, Oceanologica Acta, 15, 109–124, 1992.

Paladini de Mendoza, F., Schroeder, K., Langone, L., Chiggiato, J., Borghini, M., Giordano, P., Verazzo, G., and Miserocchi, S.: Deep-water hydrodynamic observations of two moorings sites on the continental slope of the southern Adriatic Sea (Mediterranean Sea), Earth System Science Data, 14, 5617–5635, https://doi.org/10.5194/essd-14-5617-2022, 2022.

Pisano, A., Buongiorno Nardelli, B., Tronconi, C., and Santoleri, R.: The new Mediterranean optimally interpolated pathfinder AVHRR SST Dataset (1982–2012), Remote Sensing of Environment, 176, 107–116, https://doi.org/https://doi.org/10.1016/j.rse.2016.01.019, 2016.

Pranić, P., Denamiel, C., and Vilibić, I.: Performance of the Adriatic Sea and Coast (AdriSC) climate component - A COAWST V3.3-based one-way coupled atmosphere-ocean modelling suite: Ocean results, Geoscientific Model Development, 14, 5927–5955, https://doi.org/10.5194/gmd-14-5927-2021, 2021.

Pranić, P., Denamiel, C., Janeković, I., and Vilibić, I.: Multi-model analysis of the Adriatic dense-water dynamics, Ocean Science, 19, 649–670, https://doi.org/10.5194/os-19-649-2023, 2023.

Raicich, F.: Note on the flow rates of the Adriatic rivers. Tech. Rep. 561 RF 02/94, Tech. rep., CNR Istituto Sperimentale Talassografico, Trieste, Italy, 1994.

Raicich, F.: The sea level time series of Trieste, Molo Sartorio, Italy (1869–2021), Earth System Science Data, 15, 1749–1763, https://doi.org/10.5194/essd-15-1749-2023, 2023a.

Raicich, F.: Sea level observations at Trieste, Molo Sartorio, Italy., https://doi.org/10.17882/62758, https://www.seanoe.org/data/00516/62758/, 2023b.

Raicich, F. and Colucci, R. R.: A near-surface sea temperature time series from Trieste, northern Adriatic Sea (1899-2015), Earth System Science Data, 11, 761–768, https://doi.org/10.5194/essd-11-761-2019, 2019.

Ricchi, A., Miglietta, M. M., Barbariol, F., Benetazzo, A., Bergamasco, A., Bonaldo, D., Cassardo, C., Falcieri, F. M., Modugno, G., Russo, A., Sclavo, M., and Carniel, S.: Sensitivity of a Mediterranean tropical-like Cyclone to different model configurations and coupling strategies, Atmosphere, 8, https://doi.org/10.3390/atmos8050092, 2017.

Ricchi, A., Bonaldo, D., Cioni, G., Carniel, S., and Miglietta, M. M.: Simulation of a flash - flood event over the Adriatic Sea with a high - resolution atmosphere – ocean – wave coupled system, Scientific Reports, 9388, 1–11, https://doi.org/10.1038/s41598-021-88476-1, 2021.

Samuelsson, P., Jones, C. G., Willén, U., Ullerstig, A., Gollvik, S., Hansson, U., Jansson, C., Kjellström, E., Nikulin, G., and Wyser, K.: The Rossby Centre Regional Climate model RCA3: Model description and performance, Tellus, Series A: Dynamic Meteorology and Oceanography, 63, 4–23, https://doi.org/10.1111/j.1600-0870.2010.00478.x, 2011.

Sanchez-Arcilla, A., Staneva, J., Cavaleri, L., Badger, M., Bidlot, J., Sorensen, J. T., Hansen, L. B., Martin, A., Saulter, A., Espino, M., Miglietta, M. M., Mestres, M., Bonaldo, D., Pezzutto, P., Schulz-Stellenfleth, J., Wiese, A., Larsen, X., Carniel, S., Bolaños, R., Abdalla, S., and Tiesi, A.: CMEMS-Based Coastal Analyses: Conditioning, Coupling and Limits for Applications, Frontiers in Marine Science, 8, https://doi.org/10.3389/fmars.2021.604741, 2021.

Sangelantoni, L., Sobolowski, S., Lorenz, T., Hodnebrog, Cardoso, R. M., Soares, P. M., Ferretti, R., Lavín-Gullón, A., Fernandez, J., Goergen, K., Milovac, J., Katragkou, E., Kartsios, S., Coppola, E., Pichelli, E., Adinolfi, M., Mercogliano, P., Berthou, S., de Vries, H., Dobler, A., Belušić, D., Feldmann, H., Tölle, M. H., and Bastin, S.: Investigating the representation of heatwaves from an ensemble of km-scale regional climate simulations within CORDEX-FPS convection, Climate Dynamics, https://doi.org/10.1007/s00382-023-06769-9, 2023.

Scoccimarro, E., Gualdi, S., Bellucci, A., Sanna, A., Fogli, P. G., Manzini, E., Vichi, M., Oddo, P., and Navarra, A.: Effects of Tropical Cyclones on Ocean Heat Transport in a High-Resolution Coupled General Circulation Model, Journal of Climate, 24, 4368 – 4384, https://doi.org/10.1175/2011JCLI4104.1, 2011.

Signell, R. P., Carniel, S., Cavaleri, L., Chiggiato, J., Doyle, J. D., Pullen, J., and Sclavo, M.: Assessment of wind quality for oceanographic modelling in semi-enclosed basins, Journal of Marine Systems, 53, 217–233, https://doi.org/10.1016/j.jmarsys.2004.03.006, 2005.

Sikirić, M. D., Janeković, I., and Kuzmić, M.: A new approach to bathymetry smoothing in sigma-coordinate ocean models, Ocean Modelling, 29, 128–136, https://doi.org/10.1016/j.ocemod.2009.03.009, 2009.

Simoncelli, S., Fratianni, C., Pinardi, N., Grandi, A., Drudi, M., Oddo, P., and Dobricic, S.: Mediterranean Sea Physical Reanalysis (CMEMS MED-Physics) (Version 1, Data set). Copernicus Monitoring Environment Marine Service (CMEMS), https://doi.org/10.25423/MEDSEA_REANALYSIS_PHYS_ 006_004, 2019.

SI@SIMC@ARPAE: Dext3r beta, available at: https://simc.arpae.it/dext3r/, last accessed 01 September 2022, 2022.

Taylor, K. E., Stouffer, R. J., and Meehl, G. A.: An Overview of CMIP5 and the Experiment Design, Bulletin of the American Meteorological Society, 93, 485 – 498, https://doi.org/10.1175/BAMS-D-11-00094.1, 2012.

Tojčić, I., Denamiel, C., and Vilibić, I.: Kilometer-scale trends and variability of the Adriatic present climate (1987–2017), Climate Dynamics, 61, 2521–2545, https://doi.org/10.1007/s00382-023-06700-2, 2023.

Tojčić, I., Denamiel, C., and Vilibić, I.: Kilometer-scale trends, variability, and extremes of the Adriatic far-future climate (RCP 8.5, 2070-2100), FRONTIERS IN MARINE SCIENCE, 11, https://doi.org/10.3389/fmars.2024.1329020, 2024.

Umgiesser, G., Ferrarin, C., Bajo, M., Bellafiore, D., Cucco, A., De Pascalis, F., Ghezzo, M., McKiver, W., and Arpaia, L.: Hydrodynamic modelling in marginal and coastal seas-The case of the Adriatic Sea as a permanent laboratory for numerical approach, OCEAN MODELLING, 179, https://doi.org/10.1016/j.ocemod.2022.102123, 2022.

Varga, A. J. and Breuer, H.: Sensitivity of simulated temperature, precipitation, and global radiation to different WRF configurations over the Carpathian Basin for regional climate applications, Climate Dynamics, 55, 2849–2866, https://doi.org/10.1007/s00382-020-05416-x, 2020.

Vilibić, I.: Evaluation of the AdriSC Climate Component: Ocean Results, https://doi.org/10.5281/zenodo.5707773, 2021.

Vilibić, I., Sepić, J., Pasarić, M., and Orlić, M.: The Adriatic Sea: A Long-Standing Laboratory for Sea Level Studies, PURE AND APPLIED GEOPHYSICS, 174, 3765–3811, https://doi.org/10.1007/s00024-017-1625-8, 2017.

Vilibić, I., Pranić, P., and Denamiel, C.: North Adriatic Dense Water: lessons learned since the pioneering work of Mira Zore-Armanda 60 years ago, ACTA ADRIATICA, 64, 53–78, https://doi.org/10.32582/aa.64.1.11, 2023.

Wentz, F., Scott, J., Hoffman, R., Leidner, M., Atlas, R., and Ardizzone, J.: Remote Sensing Systems Cross-Calibrated Multi-Platform (CCMP) 6-hourly ocean vector wind analysis product on 0.25 deg grid, Version 2.0. Remote Sensing Systems, Santa Rosa, CA. Available online at www.remss.com/measurements/ccmp. [Accessed 22 Dec 2023], 2015.

Woollings, T.: Dynamical influences on European climate: an uncertain future, Philosophical Transactions of the Royal Society A: Mathematical, Physical and Engineering Sciences, 368, 3733–3756, https://doi.org/10.1098/rsta.2010.0040, 2010.

Woollings, T., Barriopedro, D., Methven, J., Son, S. W., Martius, O., Harvey, B., Sillmann, J., Lupo, A. R., and Seneviratne, S.: Blocking and its Response to Climate Change, https://doi.org/10.1007/s40641-018-0108-z, 2018.

Zuliani, A., Zaggia, L., Collavini, F., and Zonta, R.: Freshwater discharge from the drainage basin to the Venice Lagoon (Italy), Environment International, https://doi.org/10.1016/j.envint.2005.05.004, 2005.

https://doi.org/10.5194/egusphere-2024-1468
Preprint. Discussion started: 30 May 2024

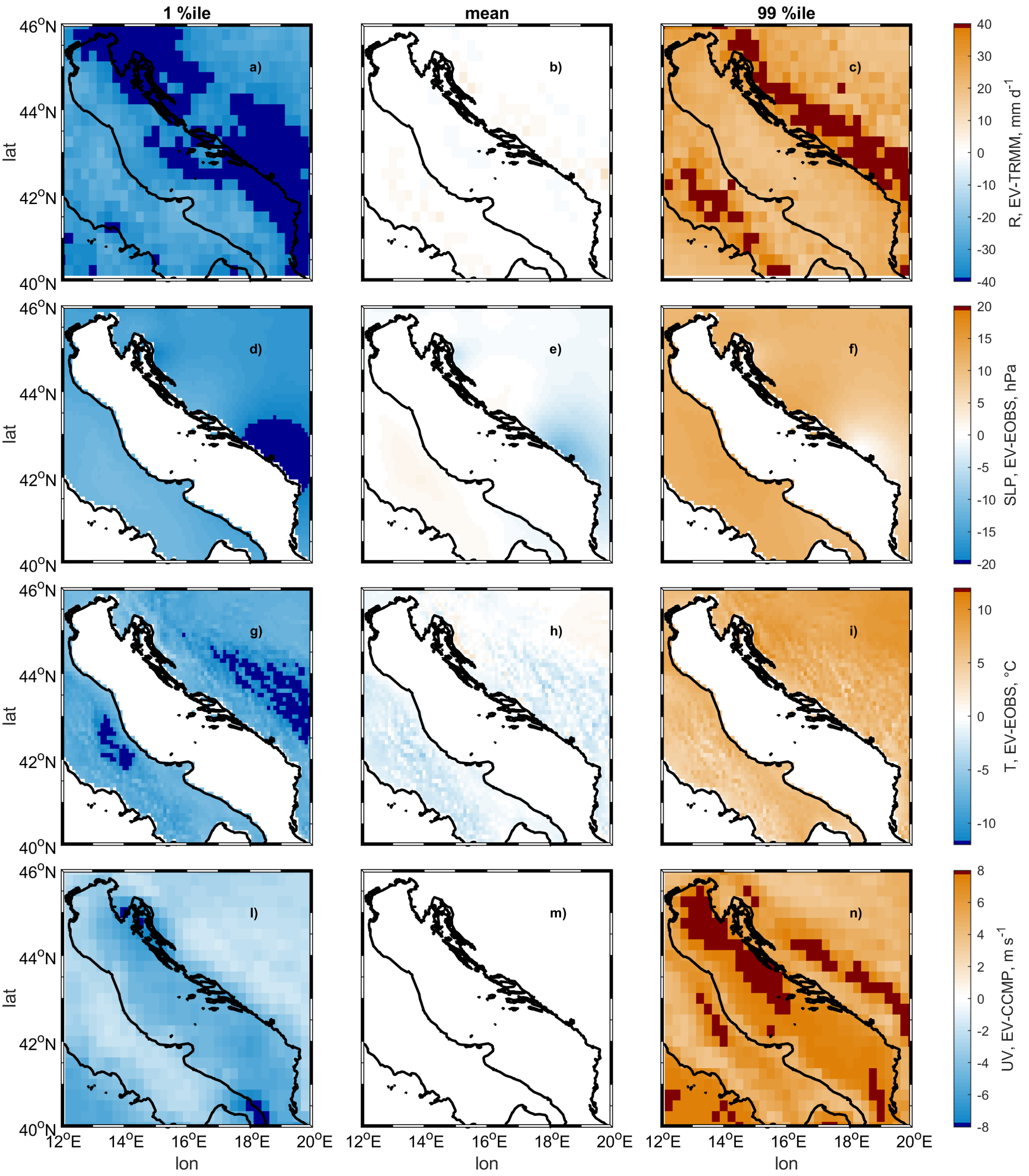

Figure 3. 1- percentile (a,d,g,l), mean (b,e,h,m), and 99- (c,f,i,n) percentile of the difference (*Bias* in Denamiel et al. 2021a) between atmospheric forcing in EV run and different gridded observational datasets.

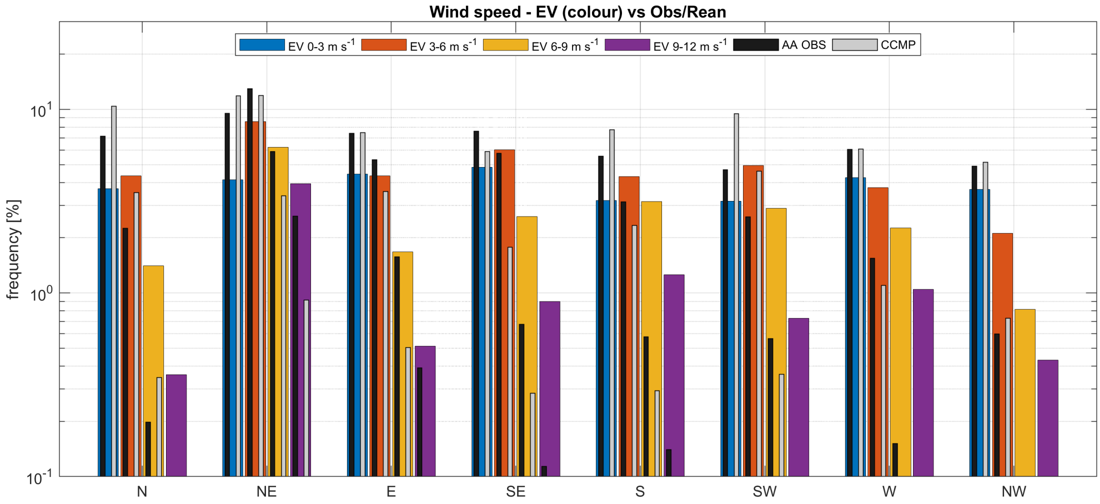

Figure 4. Comparison of SMHI-RCA4 fields used in the EV run (coloured bars) against CCMP directional wind statistics and in situ observations (gray and black bars respectively) at AA against observations in the reference period (July 10, 1987 - December 31, 2010).

https://doi.org/10.5194/egusphere-2024-1468
Preprint. Discussion started: 30 May 2024

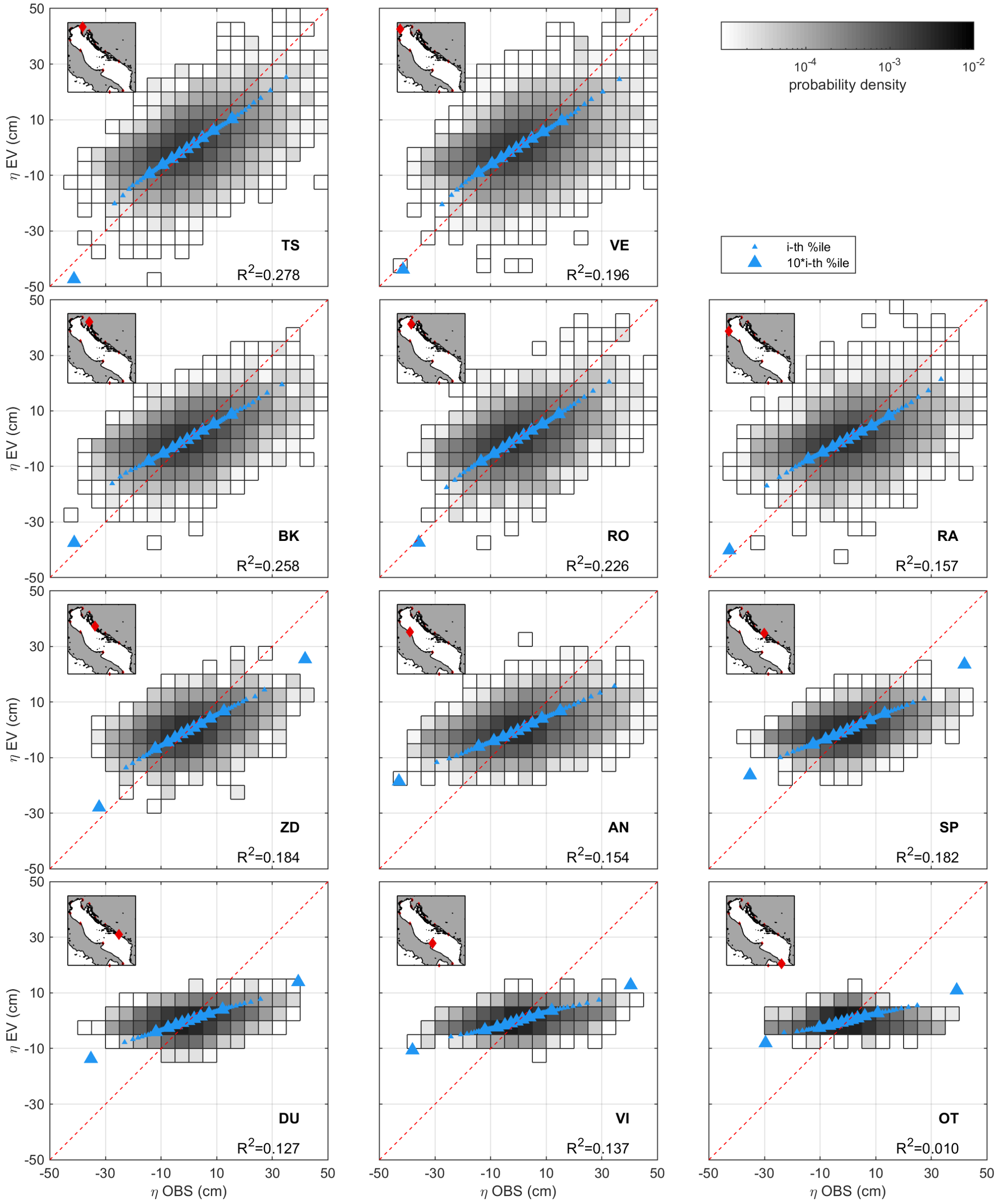

Figure 5. Scatterplots of modelled (EV) and observed (OBS) sea levels at different tide gauges and their percentiles. R^2 represents respectively the correlation coefficient for the whole series.

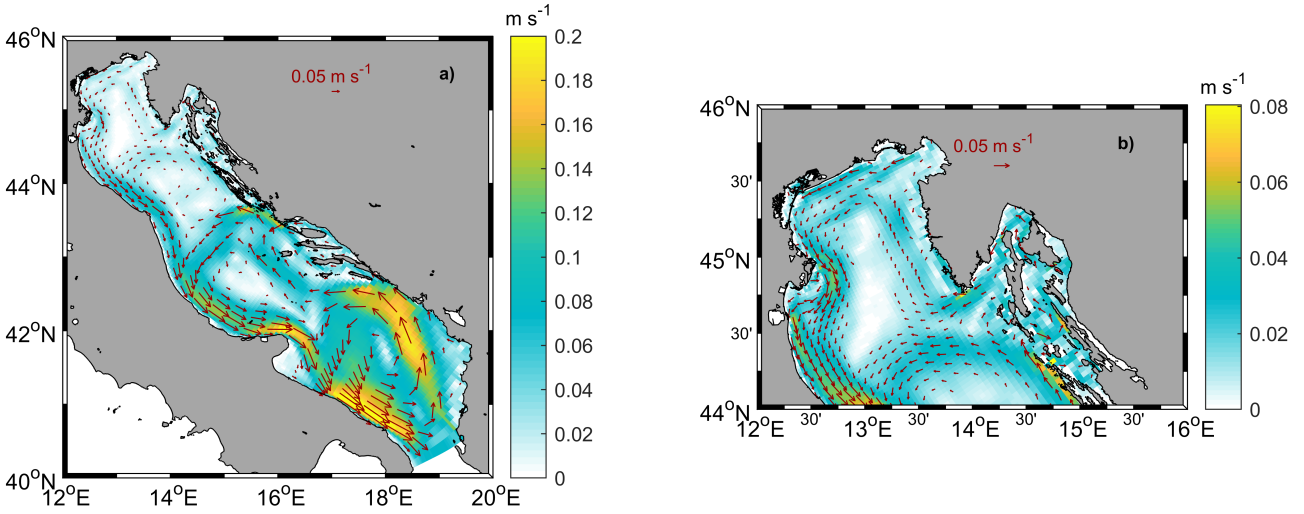

Figure 6. Mean near-surface (0-25 m) circulation patterns in the whole basin (a) and in the Northern Adriatic Sea (b) in the EV run. Vectors have been subsampled respectively every 5 and 3 grid points, omitting values smaller than 0.01 m s^{-}1.

https://doi.org/10.5194/egusphere-2024-1468
Preprint. Discussion started: 30 May 2024

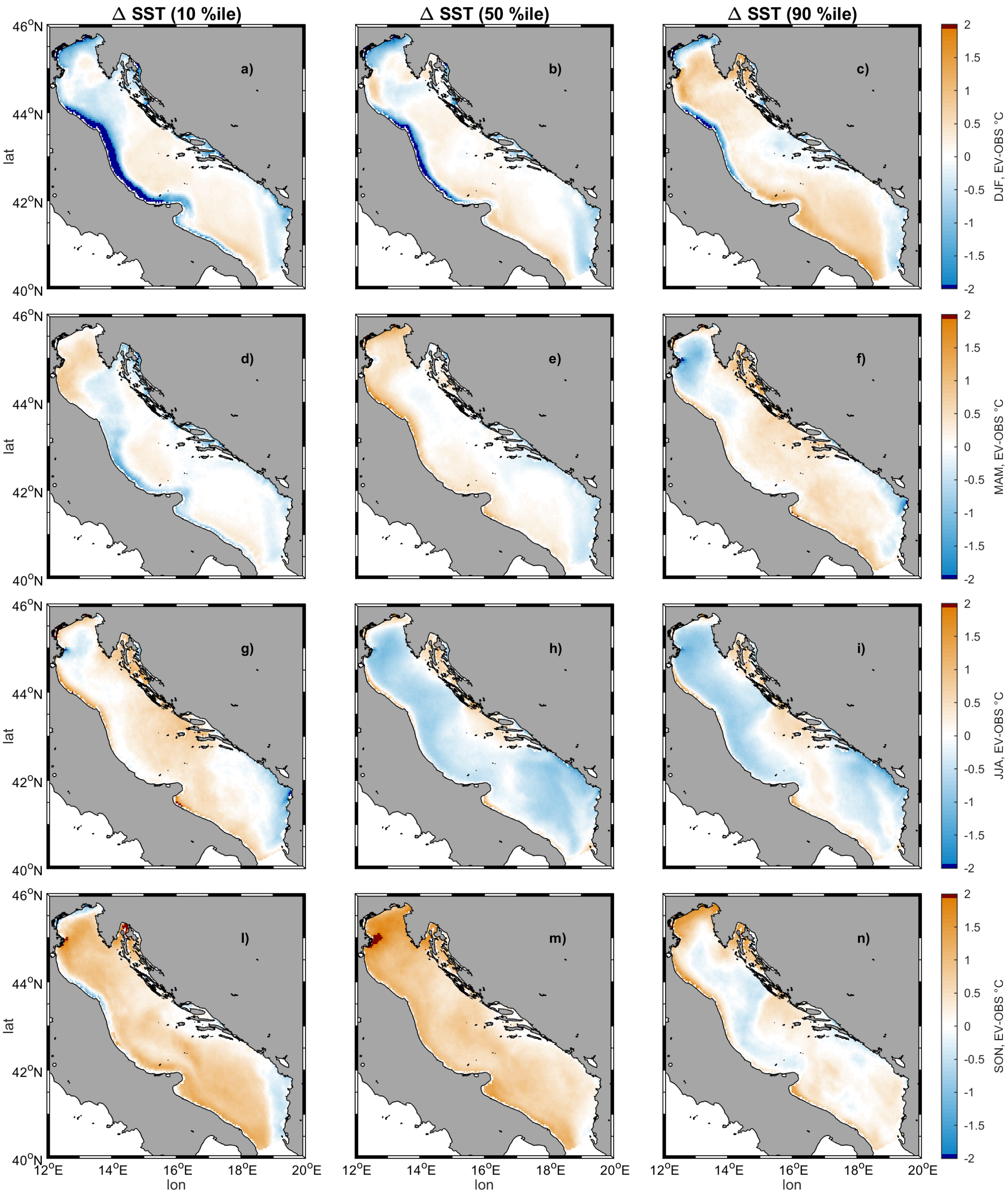

Figure 7. Patterns of difference between modelled (EV run) and observed (AVHRR) seasonal SST percentiles.

https://doi.org/10.5194/egusphere-2024-1468
Preprint. Discussion started: 30 May 2024

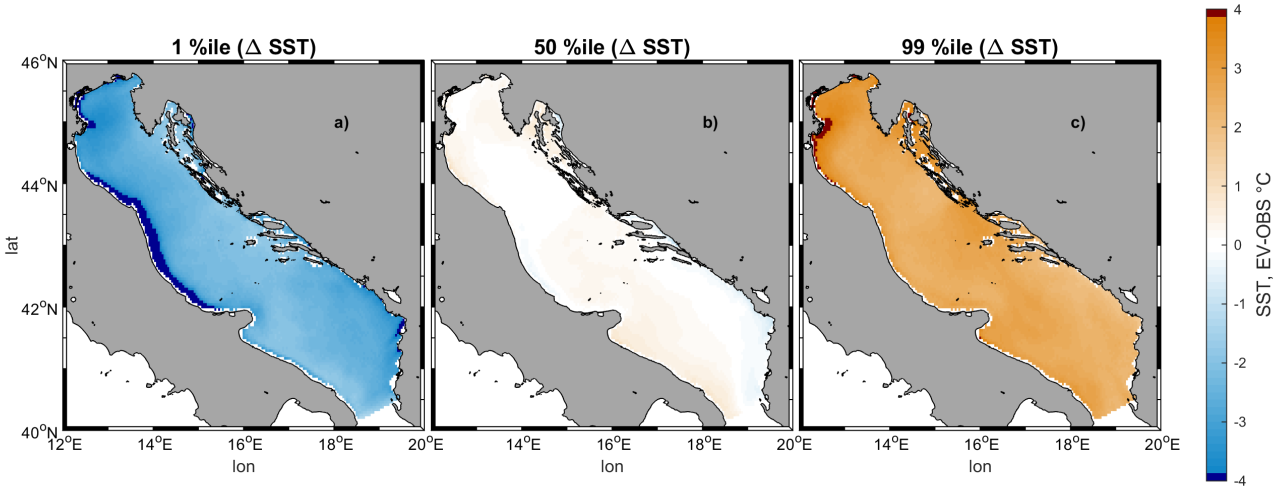

Figure 8. Percentiles (1st, 50th, and 99th) of difference between modelled (EV run) and observed seasonal SST.

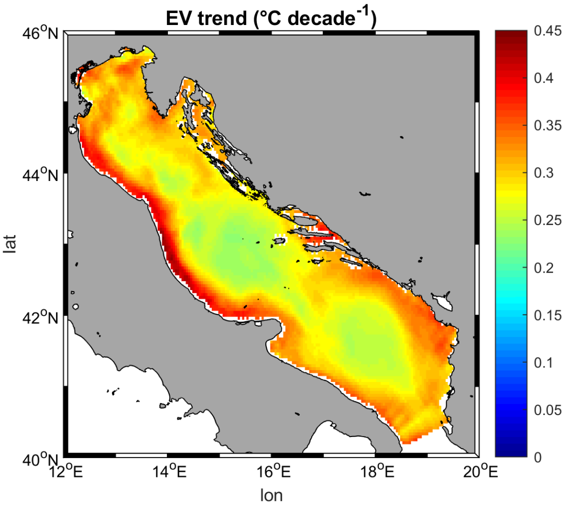

Figure 9. Modelled (EV run) SST trends in the basin, reference period 1987-2010. All values are statistically significant following a Mann-Kendall test.

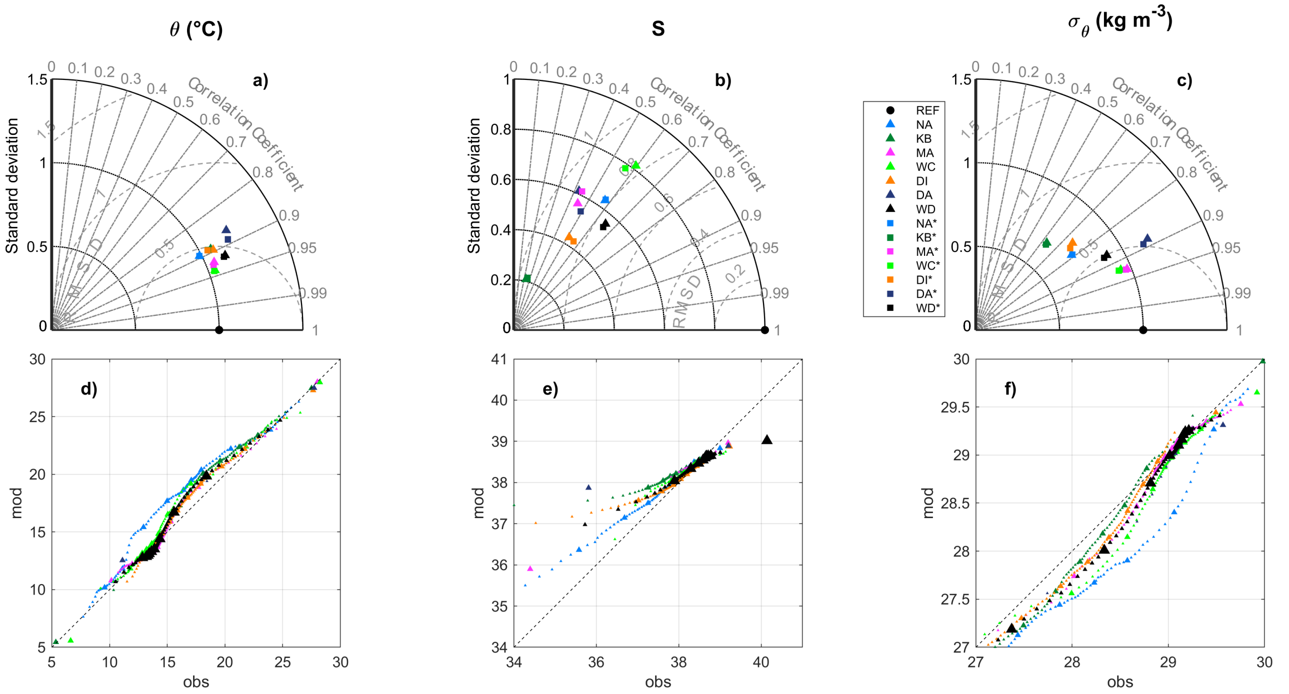

Figure 10. Overview of the EV run performance in reproducing the properties of the water structure, namely potential temperature (θ), salinity (S), and potential density anomaly (σ_θ). All plots refer to the subdomains identified in Figure 1b, i.e. Northern Adriatic (NA), Kvarner Bay (KB), Middle Adriatic (MA), Western Coast (WC), Dalmatian Islands (DI), and Deep Adriatic (DA); WB represents the Whole Basin. Panels a-c: Taylor diagrams for the EV and EV$*$ runs; Panels d-f: Q-Q plots for the EV run, with small markers every quantile and larger markers every 10 quantiles.

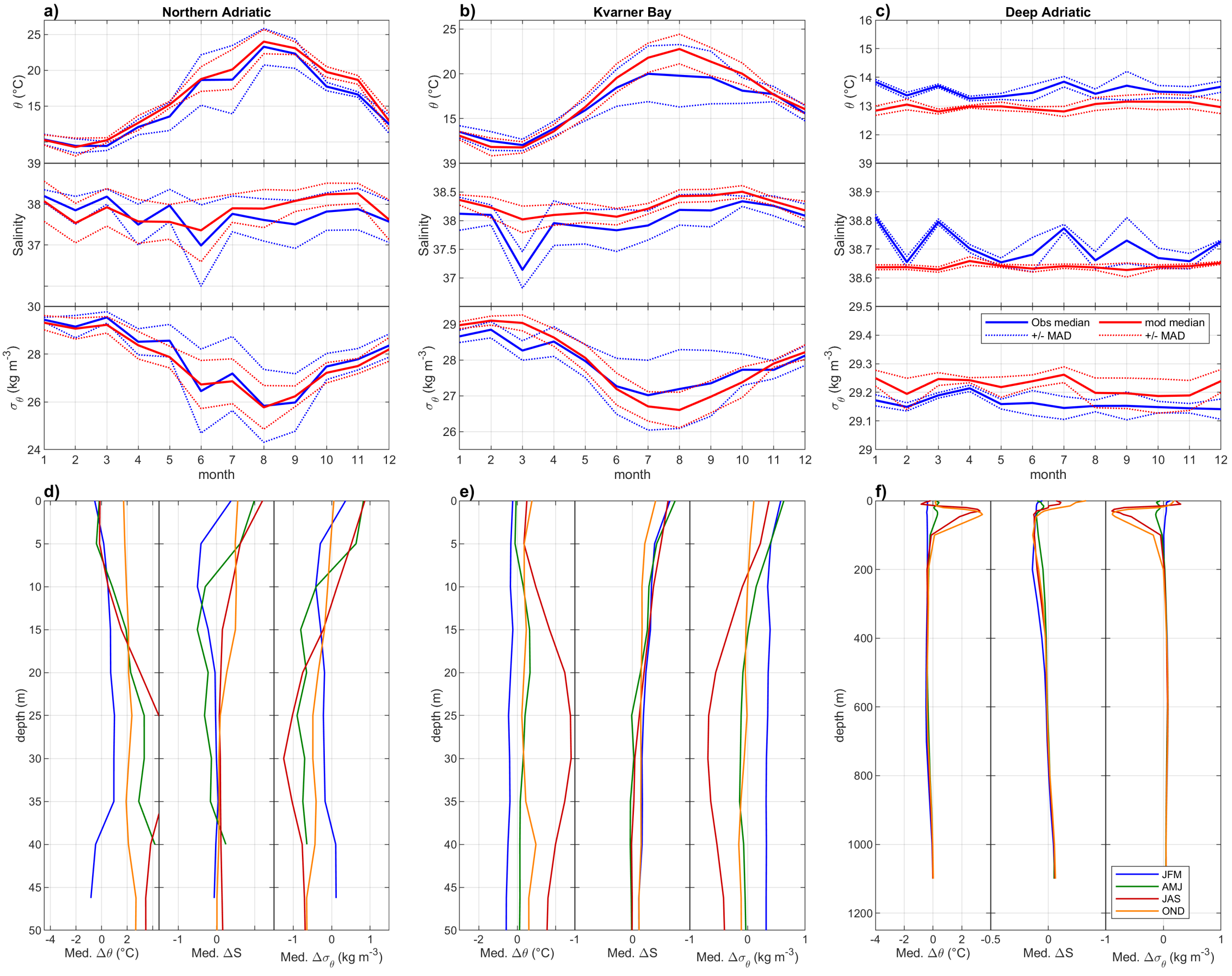

Figure 11. Monthy climatologies of modelled (EV run) and observed (CTD dataset) median potential temperature, salinity and potential density anomaly for the Northern Adriatic (a), Kvarner Bay (b), and Deep Adriatic (c). Dotted lines represent the median values ± the mean absoulte deviation (MAD) for the dataset. For the same subdomains, seasonal profiles (in this case seasons have been defined as in Pranić et al. 2021 in order to facilitate the comparison) of median mismatch between model and observations (panels d,e,f).

https://doi.org/10.5194/egusphere-2024-1468
Preprint. Discussion started: 30 May 2024

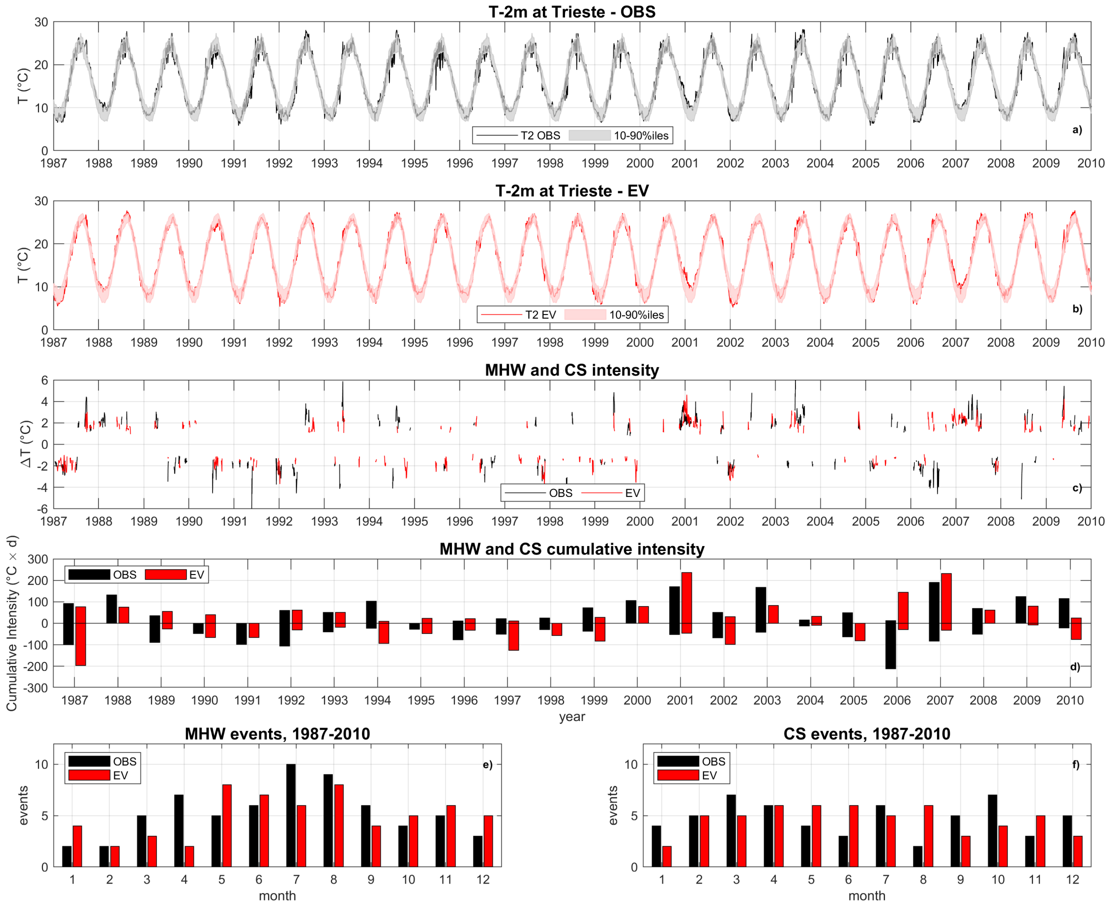

Figure 12. Comparison of modelled (EV) and observed thermal extreme events at Trieste station. Panels (a-b) represent respectively the observed and modelled time series alongside with the identification of the 10th and 90th daily percentiles for the period (here computed as a moving average within a 15-day sliding window); (c) highlights the events found in either series and their intensity; (d) compares the yearly cumulative intensity of the extreme events, and (e-f) compares for each month the observed and modelled number of MHWs and CSs respectively).

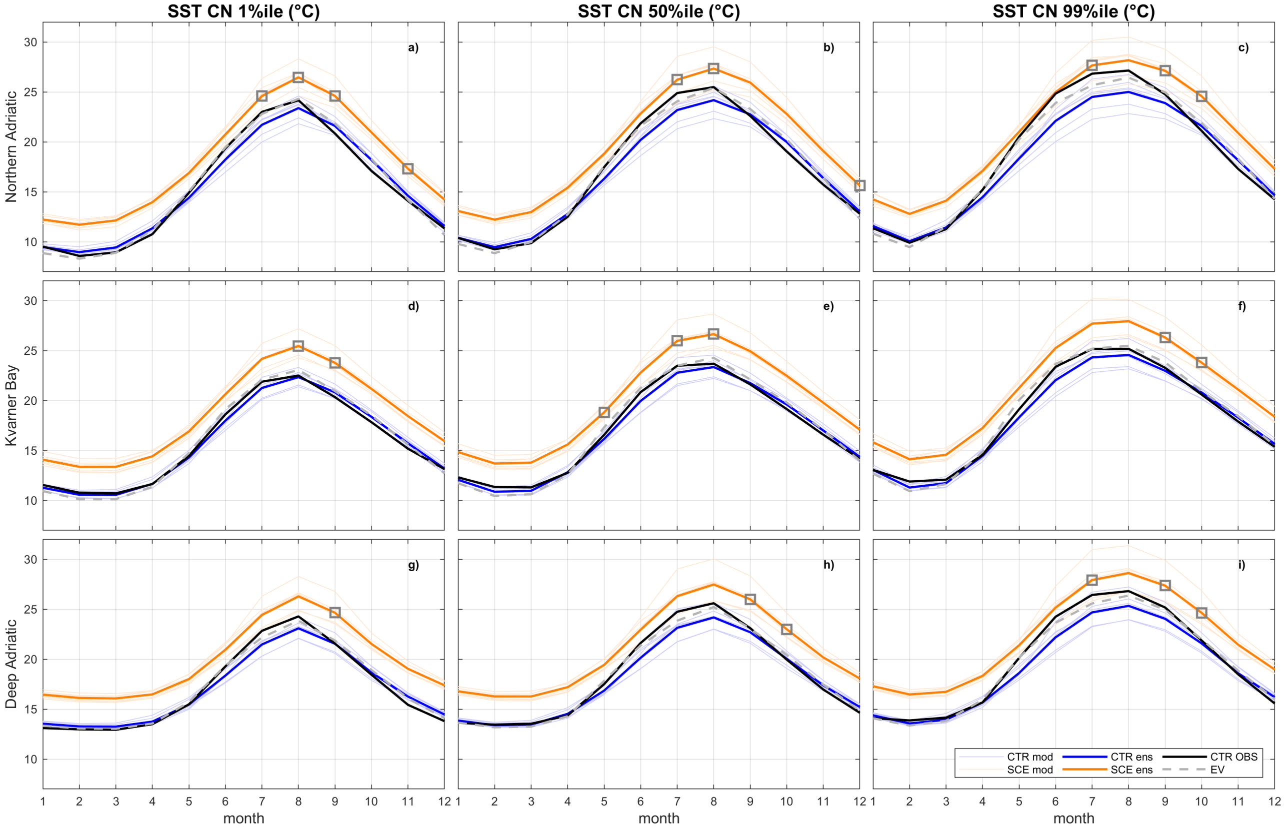

Figure 13. Modelled SST climate normals (namely, the average over the reference period) of different monthly statistics in different sub-basins under CTR (blue lines), and SCE (orange lines), where thin and thick lines represent respectively ensemble members mean, compared against observations in the historical period (black thick line) and the evaluation run (dashed gray line). Dark gray squares mark statistically non-significant variations in the ensemble distributions.

https://doi.org/10.5194/egusphere-2024-1468
Preprint. Discussion started: 30 May 2024

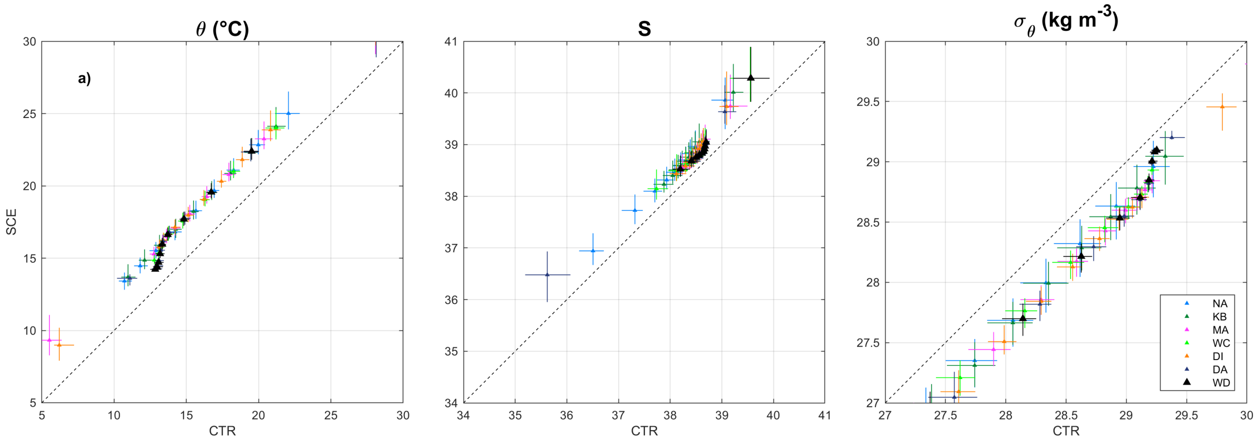

Figure 14. QQ plots representing CTR vs SCE ensemble statistics every 10 quantiles in different subdomains for potential temperature (θ), salinity (S), and potential density anomaly (σ_θ). Markers represent the ensemble mean for each considered quantile, and vertical and error bars represent the ensemble spread. The subdomains, identified in Figure 1b, are Northern Adriatic (NA), Kvarner Bay (KB), Middle Adriatic (MA), Western Coast (WC), Dalmatian Islands (DI), and Deep Adriatic (DA); WB represents the Whole Basin.

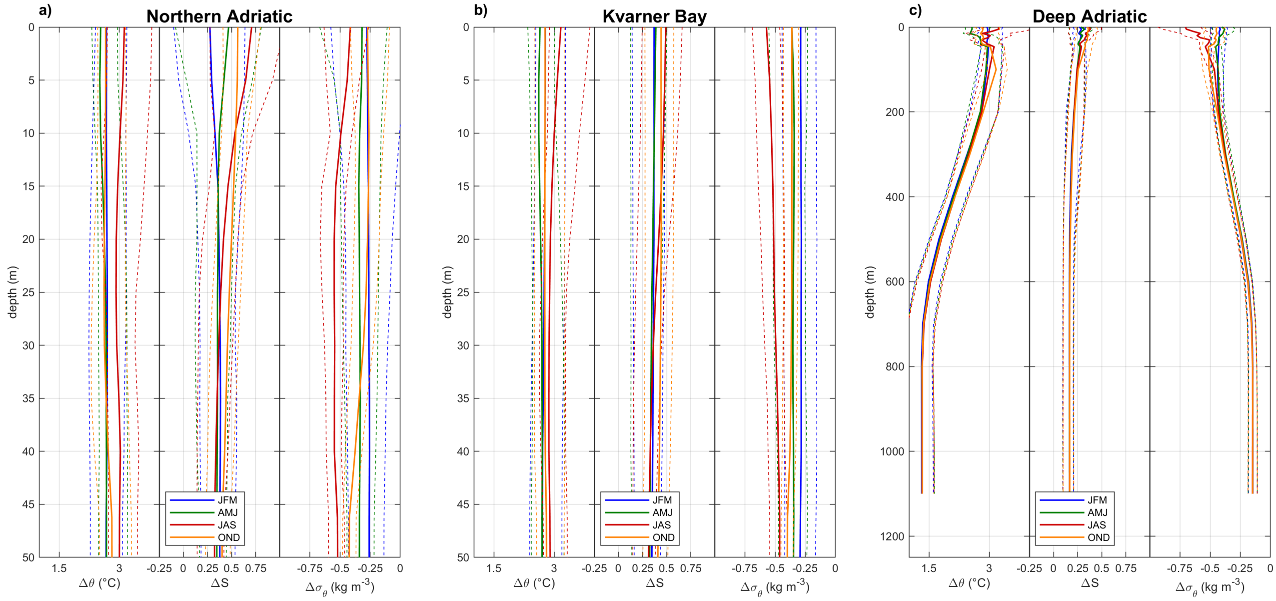

Figure 15. Variations (SCE-CTR) between median seasonal (again, with seasons defined as in Pranić et al. 2021 to enable the comparison with Figure 11) potential temperature (θ), salinity (S), and potential density anomaly (σ_θ) profiles in the Northern Adriatic (a), Kvarner Bay (b), and Deep Adriatic (c). Dashed lines bracket the ensemble spread.

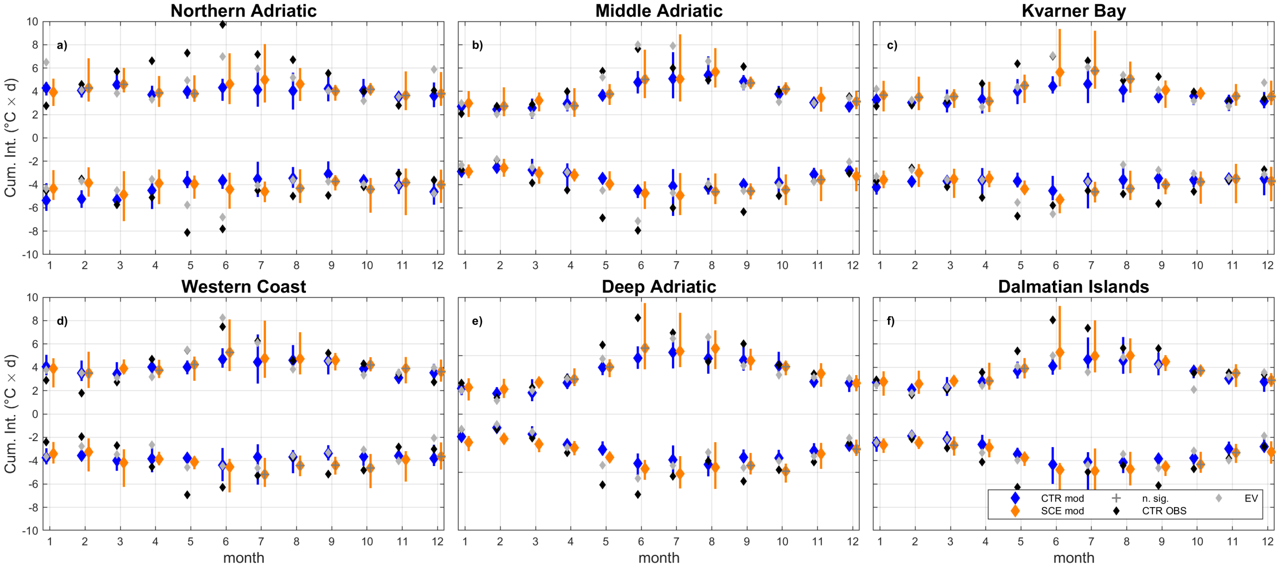

Figure 16. Monthly mean cumulative intensity of MHWs (>0) and CSs (<0) in CTR (blue markers) and SCE (orange markers), where vertical lines represent the ensemble spread, compared against the historical period (black markers) and the evaluation run (gray markers).Dark gray markers represent statistically non-significant variations in the ensemble distributions.